INSTANTONS IN QCD AND RELATED THEORIES

E. SHURYAK[1,2]

[1]Isaac Newton Institute for Mathematical Sciences,
20 Clarkson Road, Cambridge CB3 0EH, UK
[2]Physics Department*, State University of New York
Stony Brook, NY 11794, USA.

INTRODUCTION

Overview

QCD is now more than 20 years old, and naturally it has reached a certain level of maturity. Perturbative QCD has been developed in great detail, with most hard processes calculated beyond leading order, compared to data and compiled in reviews and textbooks. However, the development of non-perturbative QCD has proven to be a much more difficult task.

This is hardly surprising. While perturbative QCD could build on the methods developed in the context of QED, strategies for dealing with the non-perturbative aspects of field theories first had to be developed. The gap between hadronic phenomenology on the one side and exactly (or partly) solvable field theories is still huge. While some fascinating discoveries (instantons among them) have been made, and important insights emerged from lattice simulations and hadronic phenomenology, a lot of work remains to be done in order to unite these approaches and truly understand the phenomena involved.

In order to develop a meaningful strategy we have to first see if the problem can be split into few separate steps: as usual in physics, this may be possible if some hierarchy of scales exist. And indeed, it was found that looking at the problem from several angles that it seems to be the case. Historically the first idea about the scales of the non-perturbative physics was suggested already in the early 60's. Nambu and Jona-Lasinio[1] (NJL) have suggested a model, inspired by an analogy to superconductivity. A hypothetical four-fermion interaction was introduced in order to explain the chiral symmetry breaking, creation of pions as Goldstone bosons, etc. The scale at which all this happens enters their model as a cut-off parameter, $\Lambda_{\chi SB} \sim 1$ GeV, and this effective theory (containing pions and constituent quarks) works in the gap *between* this scale and some lower hadronic scale, presumably related to confinement. Although the progress in understanding confinement is still very slow, the fundamental mechanism of

*Permanent address.

deviations from perturbative QCD and of the chiral symmetry breaking is now clarified in significant details.

The recent comprehensive review[2] should be consulted for details (only general ideas and some results will be described below). A qualitative picture of the vacuum suggested, is as follows: the non-perturbative gluon fields are concentrated mostly in *small-size* ($\rho \sim 1/3$ fm) topological fluctuations, the instantons. These have rather strong gauge fields, thus explaining why the parameter $\Lambda_{\chi SB} \sim 1$ GeV is so surprisingly large, why the glueballs are so heavy[3], why the scalar glueball is so small in size, why ordinary hadrons may have noticeable "intrinsic charm", etc. In the physics of light quarks it is more important that instantons play a role similar to that of a phonon exchange in a superconductor, providing the fundamental mechanism for the four-fermion attractive interaction in scalar and pseudoscalar channels. It breaks the chiral symmetry and creates the quark condensate, generates the quark "constituent mass" of about 400 MeV, explains the pion properties, etc.[4, 5]. In short, it does all what the NJL interaction is supposed to do.

Instantons also do this job better, because they generate vertices with the particular non-locality related to the instanton size: so many nasty questions related with the non-renormalizable NJL model have been naturally solved. Furthermore, a numerical but practical approach was discovered, allowing to include *all* orders in the instanton-induced 't Hooft effective interaction: this is something which in NJL-based calculations has never even attempted. Furthermore, this instanton-induced interaction is *not* identical to the NJL one. It drives the famous chiral anomaly and violates the chiral $U_A(1)$ symmetry[6], *quantitatively* explaining large η' mass.

These were the main conclusions of the applications of the simplest instanton-based vacuum model, the so called Random Instanton Liquid Model[7] (RILM), in the 1980's. It is a simple ad hoc model, an ensemble with random space-time positions and orientations, with two parameters: the mean size and spacing between instantons, $\rho \sim 1/3$ fm, $R \sim 1$ fm.

At the beginning of the 90's larger-scale studies of the RILM were made, and they have shown that it works far better than can be expected. The actual calculations are based on numerical evaluation of the quark propagator in a multi-instanton gauge field, which is then plugged in the correlator and averaged over the ensemble. The correlators were calculated in the region up to distances about 1.5 fm, where they are falling by 3-5 decades. Compared to phenomenology[10] and/or lattice results[11] whenever possible, the RILM *quantitatively* describes dozens of different hadronic correlation functions, including all main mesonic and baryonic channels. In fact, agreement is not only reached at small distances (where one can use a single-instanton approximation), but also at large ones, since the low-lying hadronic states (like pion, rho, nucleon, etc.) appear to be bound in the RILM and have reasonable masses and other parameters. In particular, it was found that instanton-induced effective interactions generate spin dependent forces between quarks: producing deeply bound nucleons (octet baryons), weakly bound[8] Δ (and decuplet members) and describing spin and orbital splittings in heavy-light hadrons[9] (D,B etc.). Although the RILM has no confinement, and thus in principle should have unphysical multi-quark cuts in its spectral density, in all major correlators it has so far been practically impossible to detect any sign of this problem. Thus, in practical terms, even the simplest instanton-based model, the RILM, outperformed other approaches (such as QCD sum rules) by a huge margin. Further studies of many other problems of hadronic physics in its framework seems justified now. Those may include various form-factors, wave and structure functions, etc.

The next step was development of a self-consistent Interacting Instanton Liquid

Model (IILM). It is a statistical model with a partition function similar to QCD, with gluonic fields represented by a superposition of instantons and the fermionic determinant calculated in the subspace of instanton zero modes. (It means that all orders in the 't Hooft effective interaction are included.) It is simple enough to be solved numerically, producing very good results. Furthermore, being self-consistent it satisfy the relevant theorems (such as chiral perturbation theory and other low energy theorems) exactly. One can also use it for studies of new phases at high temperature/density or for studies of other QCD-like theories.

Let us now mention some open problems. Why the large-size instantons are not there? How to treat consistently close instanton-antiinstanton pairs? What is the relation between instantons and the abelian-projected monopoles, and what is the reason for strong correlation between them found on the lattice?

Finally, to complete the overview, let me mention that recent progress in supersymmetric gauge theories with $N = 1$ due to Seiberg[58] and $N = 2$ due to Seiberg and Witten[59] had revealed that in this theory instantons seem to be the *only* dynamics there is! When the exact solution is expanded in inverse powers of Higgs VEV a at large a, one can see that (apart of a single perturbative one-loop log) all the power terms are just multi-instanton contributions. The first two orders have been calculated[60, 61, 62] and found to be exactly right, and all higher orders will probably be calculated soon. The challenge now is to develop the "instanton liquid" for $N = 1$ and $N = 2$ SUSY theories and bridge the gap between our phenomenological knowledge in QCD and recent theoretical advances in SUSY theories.

Scales of non-perturbative QCD

QCD is now firmly established as the correct theory of the strong interactions, but most calculations are performed in the perturbative domain - hard reactions with large momentum transfer. The limits of PQCD is a fundamental input we now consider. Although the value of the QCD scale parameter entering perturbative logs (and Particle Data Tables) is $\Lambda_{\rm QCD} \sim 0.2$ GeV ~ 1 fm^{-1} (the exact value depending on the definition), the applicability of the parton model to hard processes is limited to reactions involving a scale of at least $Q \sim 1$ GeV. Where does this scale actually come from?

Another determination of the scale of non-perturbative effects in QCD is possible from below, using effective theories. The first estimate of this kind goes back to the Nambu and Jona-Lasinio model[1], inspired in the early 60's by the analogy between chiral symmetry breaking and superconductivity. It postulates a four-fermion interaction which, if it exceeds a certain strength, leads to quark condensation, the appearance of pions as Goldstone bosons, etc. The scale at which this interactions should be cut off (in order to reproduced known properties of the pion etc.) enters the model as an explicit *upper* cut-off on the momenta, $\Lambda_{\chi SB} \sim 1$ GeV.

It was further argued that the scales for chiral symmetry breaking and confinement are very different[12]: $\Lambda_{\chi SB} \gg \Lambda_{\rm conf} \sim \Lambda_{\rm QCD}$. In particular, it implies that constituent quarks (and pions) should have sizes smaller than those of typical hadrons, explaining the success of the non-relativistic quark model. This idea was developed by Georgi and Manohar[13] in a systematic fashion: they have considered the ratio of these two scales as the natural expansion parameter in chiral effective Lagrangians. They also argued that an effective theory of pions and constituent quarks is the natural description in the intermediate regime $\Lambda_{\rm conf} < Q < \Lambda_{\chi SB}$, at which models of hadronic structure operate.

Although the progress in understanding confinement is still very slow, the fundamental mechanism of chiral symmetry breaking has been clarified in significant detail.

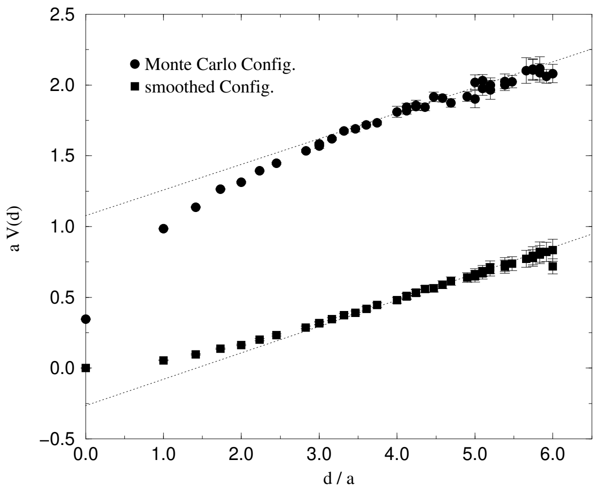

Figure 1. The $\bar{q}q$ potential before (above) and after (below) smoothening of the gauge fields, from Ref.[14].

It is the purpose of this review to explain the main ideas and results. For a more detailed exposition and technical details, the reader is invited to consult the more comprehensive work[2]. The picture of the vacuum that has emerged over the years has been termed the instanton liquid model[7].

The bottom line: it is the multiplicity, and especially the small size of instantons which explains why the strong interaction scale in QCD, $\Lambda_{\chi SB} \sim 1$ GeV, is so large as compared to $\Lambda_{\rm pert}$, the place where perturbation theory blows up.

Hadronic structure

Understanding the structure of hadrons and the regularities in the spectrum of hadrons is an old problem. Indeed, the first two attempts to understand hadronic structure, the non-relativistic quark model and current algebra, predate the development of QCD. The former still provides a very simple and phenomenologically successful scheme to describe the spectrum and the properties of hadrons, based on the idea that hadrons are loosely bound composites of massive ($\sim$ 300 MeV) constituent quarks. On the other hand, current algebra led to the conclusion that the current quark masses that appear as symmetry breaking terms in the Lagrangian are tiny, on the order of a few MeV.

To reconcile these seemingly conflicting results was one of the major challenges to model builders. Another challenging task is to understand the relative importance of the various forces acting between quarks. Hadronic models incorporate (i) perturbative one-gluon-exchange interactions, (ii) confining (string) potentials, (iii) pion or other collective exchanges and (iv) quasi-local instanton-induced interactions (which can be either two or three body forces). To understand the interplay of these interactions on the basis of hadronic spectroscopy alone is a challenging task; below we will argue that the systematic study of hadronic correlation functions is a much more appropriate tool.

Here, we only want to make a few comments on the role of these forces. First, from the study of hard processes and the analysis of correlation functions (determined from experiment or on the lattice), it has become clear that the perturbative treatment of gluon fields at the hadronic scale (1 fm = 5 GeV^{-1}) is impossible*.

*Since gluons propagate perturbatively only at distances $\ll 1$ GeV^{-1}, they effectively decouple from low energy hadronic physics.

Second, one may argue that the numerical role of confinement for the masses of hadrons made of light quarks appears to be small. It has been known for a long time that the effective confining potential that provides an optimal description of low-lying hadrons in the constituent quark model is weaker than the one deduced from heavy quark ($\bar{c}c, \bar{b}b$) states. It is tempting to attribute this difference to the extended nature of constituent quarks, in contrast to the point-like c or b quark. Constituent quarks have form-factors and only interact with sufficiently soft gluonic modes. This can be simulated on the lattice by measuring the string tension after smoothing the gauge fields. An example is shown in Fig. 1. Although the string tension (the slope at large distances) is the same for both potentials, the smoothed potential is much smaller for $r \leq 3a \sim 1$ fm. This suggests that the string potential only affects the tail of hadronic wave functions. This can be seen more explicitly by comparing hadronic correlators and wave functions in full and cooled† configurations, see[15].

There is another indirect hint that confinement effects are not dominant in light hadrons. The MIT bag model[16] assumes that confinement leads to the creation of a bubble of the perturbative phase that contains valence quarks (and gluons) surrounded by the non-perturbative vacuum in which quarks are confined. Hadronic spectroscopy then determines the difference in vacuum energy between the two phases, the so-called bag pressure. It turns out that the MIT bag constant is more than an order of magnitude smaller than the phenomenologically determined non-perturbative energy density[17]. This implies that the non-perturbative vacuum fields (e.g. instantons) are not switched off inside hadrons, and can only be slightly modified.

Over the years many hadronic models have been developed. These models cure many of the defects of the simple MIT bag model, in particularly they preserve chiral symmetry. However, relation between these models and the underlying field theory remains unclear. This is hardly surprising: hadrons are collective excitations of the vacuum, like phonons in solids, so any model that attempts to reproduce their properties without addressing the structure of the ground state is meaningless.

The strategy we wish to follow here (motivated by the hierarchy of scales discussed above) is to treat the phenomenon of chiral symmetry breaking first. Starting from a satisfactory theory of constituent quarks and pions, one can go to the next scale and try to build a quantitative theory of hadrons. We will argue that the physics of chiral symmetry breaking is quite well understood, while the physical nature of confinement remains unclear. However, given the arguments above, this should provide a reasonable approximation for hadrons made of light quarks.

The importance of instantons in the context of chiral symmetry breaking is related to the fact that the Dirac operator has a chiral zero mode in the field of an instantons. These zero modes correspond to localized quark states that can become collective if many instantons and anti-instantons interact. The resulting de-localized state corresponds to the wave function of the quark condensate. In addition to that, instanton zero modes generate an effective four fermion interaction.

This brings us back to one of the oldest approaches to hadronic structure, the already mentioned NJL model. Nambu and Jona-Lasinio showed that a short-range attractive force between fermions, if strong enough, can rearrange the vacuum and the ground state becomes superconducting. There is a gap in the fermionic spectrum, corresponding to the constituent quark mass, and a non-zero quark condensate. The role of instantons in QCD (similar to that of phonon exchange in a superconductor) is to provide the fundamental mechanism for the four-fermion interaction. Instantons fix the strength of the interaction and its spin-isospin dependence. In addition to that,

†Cooling is a specific smoothing method designed to isolate instanton contributions.

asymptotic freedom and the finite size of instantons provide a natural cutoff (as opposed to the ad hoc cutoff in the NJL model).

How to calculate?

In this lectures there is no place for technical details, which may be found in the original papers. Rather we try to explain the logical structure and possible alternatives of the theory. For that reason, discussion of possible methods to calculate something with instantons is put into the introduction, with only results of the calculation reported below.

In the QCD partition function there are two types of fields, gluons and quarks, and so the first question one addresses is which integral to take first.

(i) One way is to eliminate *gluonic* degrees of freedom first. Physical motivation for that may be that gluonic states are heavy and an effective fermionic theory should be better suited to derive an effective low-energy theory. In the instanton framework, this approach was started by 't Hooft who discovered that instantons lead to new effective interactions between light quarks. We will present the explicit form of such four-fermion interaction for two-flavor QCD below.

It is a well-trotted path and one can follow it along the development for a similar four-fermion theory, the NJL model. One can do simple mean field or random field approximation (RPA) diagrams, and find the mean condensate and properties of the mesons. Unfortunately, it is difficult to do more. For example, baryons are states with three quarks, and using quasi-local four-fermion Lagrangians for the three body problem is technically a very difficult (although solvable) quantum mechanical problem. There were no attempts to sum more complicated diagrams.

(ii) The opposite strategy can be to do fermion integral first. It is a simple step, because they only enter quadratically, leading to a fermionic determinant. This is the way lattice people proceed. In the instanton approximation, it leads to the Interacting Instanton Liquid Model, defined by the following partition function:

$$Z = \sum_{N_+,\,N_-} \frac{1}{N_+! N_-!} \int \prod_i^{N_+ + N_-} [d\Omega_i \; d(\rho_i)] \exp(-S_{\rm int}) \prod_f^{N_f} \det(\hat{D} + m_f)\,, \qquad (1)$$

describing a system of pseudo-particles interacting via the bosonic action and the fermionic determinant. Here $d\Omega_i = dU_i \, d^4 z_i \, d\rho_i$ is the measure in color orientation, position and size, associated with single instantons and $d(\rho)$ is the single instanton density $d(\rho) = dn_{I,\bar{I}}/d\rho d^4 z$ (see (21) furtheron).

The gauge interaction between instantons is approximated by a sum of pure two-body interaction $S_{\rm int} = \frac{1}{2}\sum_{I\neq J} S_{\rm int}(\Omega_{IJ})$. Genuine three body effects in the instanton interaction are not important as long as the ensemble is reasonably dilute. Implementation of this part of the interaction (quenched simulation) is quite analogous to usual statistical ensembles made of atoms.

As already mentioned, quark exchanges between instantons are included in the fermionic determinant. Finding a diagonal set of fermionic eigenstates of the Dirac operator is similar to what people are doing, e.g., in quantum chemistry when electron states for molecules are calculated. The difficulty of our problem is however much higher, because this set of fermionic states should be determined for *all* configurations which appear during the Monte-Carlo process.

If the set of fermionic states is however limited to the subspace of instanton zero modes, the problem becomes tractable numerically. Typical calculations in the IILM involved up to N$\sim$ 100 instantons/anti-instantons: it means that the determinants of

$N \times N$ matrices are involved. Such determinants can be evaluated by the ordinary workstation (and even PC these days) so quickly, that straightforward Monte Carlo simulation of IILM is possible in a matter of minutes. On the other hand, expanding the determinant in a sum of products of matrix elements, one can easily identify the sum of all closed loop diagrams up to order N in the 't Hooft interaction. Thus, in this way we take care of (practically) all orders!

Now that we know how to proceed, what should we actually calculate?

Correlators as a bridge between PQCD and hadronic physics

In a (relativistic) field theory, correlation functions of gauge invariant local operators are the proper tool to study the spectrum of the theory. The correlation functions can be calculated either from the physical states (mesons, baryons, glueballs) or in terms of the fundamental fields (quarks and gluons) of the theory. In the latter case, we have a variety of techniques at our disposal, ranging from perturbative QCD, the operator product expansion (OPE), to models of QCD and ultimately to lattice simulations. For this reason, correlation functions provide a bridge between hadronic phenomenology on the one side and the underlying structure of the QCD vacuum on the other side.

Loosely speaking, hadronic correlation functions play the same role for understanding the forces between quarks as the NN scattering phase did in the case of nuclear forces. In the case of quarks, however, confinement implies that we cannot define scattering amplitudes in the usual way. Instead, one has to focus on the behavior of gauge invariant correlation functions at short and intermediate distance scales. The available theoretical and phenomenological information about these functions was recently reviewed in[10].

Euclidean point-to-point correlation functions are defined as

$$\Pi_h(x) = \langle 0|j_h(x)j_h(0)|0\rangle, \tag{2}$$

where $j_h(x)$ is a local operator with the quantum numbers of a hadronic state h. We will concentrate on mesonic and baryonic currents of the type

$$j_{\mathrm{mes}}(x) = \delta^{ab}\bar\psi^a(x)\Gamma\psi^b(x), \tag{3}$$
$$j_{\mathrm{bar}}(x) = \epsilon^{abc}(\psi^{aT}(x)C\Gamma\psi^b(x))\Gamma'\psi^c(x). \tag{4}$$

Here, a, b, c are color indices and Γ, Γ' are isospin and Dirac matrices. In the following, we will only consider space-like separations $\tau = \sqrt{-x^2}$. In this case, correlation functions are exponentially suppressed rather than oscillatory at large distance.

Hadronic correlation functions can be written in terms of the spectrum and the coupling constants of the physical excitations with the quantum numbers of the current j_h. This connection is based on the standard dispersion relation

$$\Pi(Q^2) = \frac{1}{\pi}\int ds\, \frac{\mathrm{Im}\Pi(s)}{s+Q^2} + a_0 + a_1 Q^2 + \ldots, \tag{5}$$

(where $Q^2 = -q^2$ is the Euclidean momentum transfer and we have indicated possible subtraction constants a_i) and the spectral decomposition ($\rho(s) \equiv \frac{1}{\pi}\mathrm{Im}\Pi(s)$)

$$\rho(s=-q^2) = (2\pi)^3\sum_n \delta^4(q-q_n)\langle 0|j_h(0)|n\rangle\langle n|j_h^\dagger(0)|0\rangle. \tag{6}$$

A spectral representation of the coordinate space correlation function is obtained by Fourier transforming (5),

$$\Pi(\tau) = \int ds\, \rho(s) D(\sqrt{s},\tau), \tag{7}$$

where $D(m,\tau) = mK_1(m\tau)/(4\pi^2\tau)$ is the Euclidean propagator of a scalar particle with mass m. Note that for large arguments the correlation function decays exponentially, $\Pi(\tau) \sim \exp(-m\tau)$, where the decay is governed by the lowest pole in the spectral function.

Correlation functions that involve quarks fields only (like the meson and baryon currents introduced above) can be expressed in terms of the full quark propagator. For an isovector meson current $j_{I=1} = \bar{u}\Gamma d$ (where Γ is only a Dirac matrix), the correlator only has a "one-loop" contribution ($S^{ab}(x,y)$ is the quark propagator)

$$\Pi_{I=1}(x) = \langle \mathrm{Tr}\left[S^{ab}(0,x)\Gamma S^{ba}(x,0)\Gamma\right]\rangle. \tag{8}$$

The averaging is performed over all gauge configurations, with the weight function $\det(i\not{D} + im)\exp(-S)$. Correlators of isosinglet meson currents $j_{I=0} = \frac{1}{\sqrt{2}}(\bar{u}\Gamma u + \bar{d}\Gamma d)$ receive an additional two-loop, or disconnected, contribution

$$\begin{aligned}\Pi_{I=0}(\tau) = \langle \mathrm{Tr}\left[S^{ab}(0,x)\Gamma S^{ba}(x,0)\Gamma\right]\rangle - \\ 2\langle \mathrm{Tr}\left[S^{aa}(0,0)\Gamma\right]\,\mathrm{Tr}\left[S^{bb}(x,x)\Gamma\right]\rangle.\end{aligned} \tag{9}$$

Analogously, baryon correlators can be expressed as vacuum averages of three quark propagators.

At short distance, asymptotic freedom implies that the correlation functions are determined by free quark propagation, $S^{ab}(x,y) = \delta_{ab}S_0(x-y)$. Using the free quark propagator $S_0(x) \sim (\gamma\cdot x)/x^4$, we conclude that mesonic and baryonic correlation functions at short distance behave as $\Pi_{\mathrm{mes}} \sim 1/x^6$ and $\Pi_{\mathrm{bar}} \sim 1/x^9$, respectively. Deviations from asymptotic freedom at intermediate distances can be studied using the operator product expansion (OPE). The OPE systematically accounts for the interaction with non-perturbative quark and gluon condensates. Historically, QCD sum rules based on the OPE played an important role in establishing the connection between hadronic phenomenology and the structure of the QCD vacuum.

There are a number of sources for phenomenological information about hadronic correlation functions[10]. The ideal situation is that the spectral function is determined from the optical theorem and an experimentally accessible cross section, as in the case of the vector-isovector (rho meson) channel from $\sigma(e^+e^- \to (I = 1 \text{ hadrons}))$ and in the a_1 channel from hadronic decays of the τ lepton, $\Gamma(\tau \to \nu_\tau + \text{hadrons})$. In most cases, the information is much more limited and only the contribution of a few resonances is known. The high energy behavior, of course, can always be extracted from perturbation theory. Ultimately, the best source of information about hadronic correlation functions comes from the lattice. At present, most lattice calculations use complicated nonlocal sources, but some studies of correlation functions of local sources have been reported[18, 11].

Concluding this section, we would like to emphasize that any model of the QCD vacuum or of hadronic structure should be compared to the available information on hadronic correlation functions. Only in this way can the structure of hadrons and the effective forces between quarks be connected to the structure the QCD vacuum.

INSTANTONS

Instantons and tunneling

In this section we remind the reader of a few basic facts about instantons. All of this material can be found in reviews or text books, see for example[19, 20, 2]. Instantons are solutions of the classical equations of motion in imaginary (or Euclidean) time. This means that, unlike solitons, instantons are not physical objects in Minkowski space, but tunneling paths that connect different vacua of the theory.

"Tunneling" phenomena in quantum mechanics were discovered by George Gamow in the late 20's in the context of alpha decay of nuclei. He explained one of the *mysteries of radioactivity*: why the alpha clusters, formed inside the nuclei, should hit its walls each 10^{-22} sec or so, for a time as long as sometimes billions of years, in order to get their freedom. He emphasized in his multiple lectures and popular books how unusual quantum tunneling is, being so orthogonal to classical mechanics. And still, it is possible to use *classical mechanics* for the description of classically forbidden phenomena!

An instanton is precisely a *classical path through a barrier*, so one can understandably raise the question of how it can work. In quantum mechanics, as in classical mechanics, energy is conserved and the Schrödinger equation can be understood as

$$E = \frac{\langle p^2 \rangle}{2m} + \langle V(x) \rangle \tag{10}$$

In the classically allowed region, $p^2 > 0$ and the wave function is a wave $\psi \sim \exp(ipx)$ with real p. However, if we are in the classically forbidden region $E < V$, so we must have negative kinetic energy or *imaginary* p.

In quantum mechanics this simply means that the wave function decays with distance, $\psi \sim \exp(-|p|x)$. If so, one is able to understand why tunneling is such a rare event. Now, if p is imaginary, why not try to interpret it as *motion in imaginary time*? Changing t to $\tau = it$, we have the new classical equation of motion, with an opposite sign for the force:

$$m\frac{d^2x}{d\tau^2} = -F = -\frac{d(-V)}{dx}. \tag{11}$$

This is the same as flipping the potential upside down! Thus classical paths describing tunneling do exist, though in imaginary time.

In quantum field theory instantons also appear as a sub-barrier path, being extremas of the (euclidean) QCD partition function

$$Z = \int DA_\mu \, \exp(-S) \prod_f^{N_f} \det\left(i\not{D} + im_f\right), \tag{12}$$

$$S = \frac{1}{4g^2}\int d^4x \, G^a_{\mu\nu} G^a_{\mu\nu}. \tag{13}$$

Here, S is the gauge field action and the determinant of the Dirac operator $i\not{D} = i\gamma_\mu(\partial_\mu - iA_\mu)$ accounts for the contribution of fermions. In the semi-classical approximation, we look for saddle points of the functional integral (12), i.e. configurations that minimize the classical action S. This means that saddle point configurations are solutions of the classical equations of motion.

These solutions can be found using the identity

$$S = \frac{1}{4g^2}\int d^4x \left[\pm G^a_{\mu\nu}\tilde{G}^a_{\mu\nu} + \frac{1}{2}\left(G^a_{\mu\nu} \mp \tilde{G}^a_{\mu\nu}\right)^2\right], \tag{14}$$

where $\tilde{G}_{\mu\nu} = \frac{1}{2}\epsilon_{\mu\nu\rho\sigma}G_{\rho\sigma}$ is the dual field strength tensor (the field strength tensor in which the roles of electric and magnetic fields are reversed). Since the last term is always positive, it is clear that the action is minimal if the field is (anti) self-dual

$$G^a_{\mu\nu} = \pm\tilde{G}^a_{\mu\nu}. \tag{15}$$

The action of a self-dual field configuration is determined by its topological charge

$$Q = \frac{1}{32\pi^2}\int d^4x\, G^a_{\mu\nu}\tilde{G}^a_{\mu\nu}. \tag{16}$$

From (14) we have $S = (8\pi^2|Q|)/g^2$. For finite action configurations, Q has to be an integer. The instanton is a solution with[21] $Q = 1$

$$A^a_\mu(x) = \frac{2\eta_{a\mu\nu}x_\nu}{x^2+\rho^2}, \tag{17}$$

where the 't Hooft symbol $\eta_{a\mu\nu}$ is defined by

$$\eta_{a\mu\nu} = \begin{cases} \epsilon_{a\mu\nu} & \mu,\,\nu = 1,\,2,\,3, \\ \delta_{a\mu} & \nu = 4, \\ -\delta_{a\nu} & \mu = 4. \end{cases} \tag{18}$$

and ρ is an arbitrary parameter characterizing the size of the instanton. The classical instanton solution has a number of degrees of freedom, known as collective coordinates. In addition to the size, the solution is characterized by the instanton position z_μ and the color orientation matrix R^{ab} (corresponding to color rotations $A^a_\mu \to R^{ab}A^b_\mu$). A solution with topological charge $Q = -1$ can be constructed by replacing $\eta_{a\mu\nu} \to \overline{\eta}_{a\mu\nu}$, where $\overline{\eta}_{a\mu\nu}$ is defined by changing the sign of the last two equations in (18).

The physical meaning of the instanton solution becomes clear if we consider the classical Yang-Mills Hamiltonian (in the temporal gauge, $A_0 = 0$)

$$H = \frac{1}{2g^2}\int d^3x\,(E_i^2 + B_i^2), \tag{19}$$

where E_i^2 is the kinetic and B_i^2 the potential energy term. The classical vacua corresponds to configurations with zero field strength. For non-abelian gauge fields this limits the gauge fields to be "pure gauge" $A_i = iU(\vec{x})\partial_i U(\vec{x})^\dagger$. Such configurations are characterized by a topological winding number n_W which distinguishes between gauge transformations U that are not continuously connected to the identity.

This means that there is an infinite set of classical vacua enumerated by an integer n. Instantons are tunneling solutions that connect the different vacua. They have potential energy $B^2 > 0$ and kinetic energy $E^2 < 0$, their sum being zero at any moment in time. Since the instanton action is finite, the barrier between the topological vacua can be penetrated, and the true vacuum is a linear combination $|\theta\rangle = \sum_n e^{in\theta}|n\rangle$, called the theta vacuum. In QCD, the value of θ is an external parameter. If $\theta \neq 0$ the QCD vacuum breaks CP invariance. Experimental limits on CP violation require* $\theta < 10^{-9}$.

The *rate* of tunneling between different topological vacua will from now on be called the "instanton density" n (in space-time). It is determined by the semi-classical (WKB) method. From the single instanton action one expects

$$P_{\rm tunneling} \sim \exp(-8\pi^2/g^2). \tag{20}$$

The factor in front of the exponent can be determined by taking into account fluctuations $A_\mu = A^{cl}_\mu + \delta A_\mu$ around the classical instanton solution. This calculation was performed by 't Hooft in a classic paper[22]. The result is

$$dn_I = \frac{0.47\exp(-1.68N_c)}{(N_c-1)!(N_c-2)!}\left(\frac{8\pi^2}{g^2}\right)^{2N_c}\exp\left(-\frac{8\pi^2}{g^2(\rho)}\right)\frac{d^4z\,d\rho}{\rho^5}, \tag{21}$$

*The question why θ happens to be so small is known as the "strong CP problem". Most likely, the resolution of the strong CP problem requires physics outside QCD and we will not discuss it any further.

where $g^2(\rho)$ is the running coupling constant at the scale of the instanton size. Taking into account quantum fluctuations, the effective action depends on the instanton size. Using the one-loop beta function the result can be written as $dn_I/(d^4z) \sim d\rho\, \rho^{-5}(\rho\Lambda)^b$ where $b = (11N_c/3) = 11$ is the first coefficient of the beta function. Since b is a large number, small size instantons are strongly suppressed. On the other hand, there appears to be a divergence at large ρ (where the perturbative analysis based on the one loop beta function is not applicable).

The instanton liquid

Above we concentrated on the effects of a single instanton, but in order to understand the structure of the QCD vacuum we have to consider ensembles with a finite density (N/V) of instantons and anti-instantons. The repulsive interaction between them provides us with a method to deal with large size instantons. The instanton ensemble is described by the partition function in the space of collective coordinates (1). It is a typical statistical mechanics system, described by four-dimensional pseudo-particles interacting via the bosonic interaction $S_{\rm int}$ and the (non-local) fermion determinant $\det(i\not{D}+im_f)$. This means that we can evaluate the partition function using standard techniques of statistical mechanics.

The simplest method is the mean field approximation. If we ignore all correlations among instantons, the partition function can be represented in terms of a single instanton distribution[23] $\mu(\rho)$

$$Z \simeq \frac{1}{N_+!N_-!}\left(V\int d\rho\,\mu(\rho)\right)^{N_++N_-}. \tag{22}$$

For small ρ, the instanton distribution is given by the single instanton result (21) while for larger ρ interactions are important and the size distribution is modified. If the average effective interaction between instantons is repulsive, large instantons are suppressed and the distribution is peaked at some average size $\bar\rho$. Precisely how to define the interaction between very close (or very large) instantons is not very well understood.

Let us mention a few simple consequences of the instanton liquid model. First, we would like to consider the gluon condensate. The volume integral of $G^2_{\mu\nu}$ in the field of a single instanton is $32\pi^2$, independent of the size of the instanton. If we can ignore interactions between instantons, we get

$$\langle G^2_{\mu\nu}\rangle = (32\pi^2)\left(\frac{N}{V}\right). \tag{23}$$

Due to tunneling, the energy density of the QCD vacuum is less than that of the perturbative vacuum (which we take to be zero). The classical energy density inside an instanton is zero everywhere (this is true for any self-dual field configuration), but quantum mechanically this result is modified

$$\epsilon = -\frac{b}{4}\left(\frac{N}{V}\right). \tag{24}$$

where b is the first coefficient of the beta function. This means that the energy density of the non-perturbative vacuum is about 1 $\mathrm{GeV/fm^3}$ lower than in the perturbative one. (Note that it is about 20 time larger than the original MIT bag constant!)

The topological susceptibility is related to fluctuations of the topological charge. The average topological charge $\langle Q\rangle = \langle(N_+-N_-)\rangle$ vanishes. In pure gauge theory, the instanton ensemble is fairly random and local fluctuations of the number of pseudo-particles are Poissonian. This means that $(N_+ - N_-) \sim \sqrt{N}$ and

$$\chi_{\rm top} = \lim_{V\to\infty} \frac{\langle Q^2\rangle}{V} = \lim_{V\to\infty} \frac{\langle (N_+ - N_-)^2\rangle}{V} \simeq \left(\frac{N}{V}\right). \tag{25}$$

In the presence of light quarks, the situation is more complicated. Light quarks lead to correlations between instantons and anti-instantons and the topological charge is screened, $\chi_{\rm top} \simeq m\langle\bar{q}q\rangle$, and vanishes in the chiral limit.

Phenomenology of the instanton liquid

The first attempt to estimate the instanton density phenomenologically was made in[24]. These authors used the value of the gluon condensate $\langle 0|(G^a_{\mu\nu})^2|0\rangle \simeq 0.5\,{\rm GeV}^4$ obtained from a QCD sum rule analysis of the charmonium spectrum[25]. If the gluon condensate is dominated by (weakly interacting) instantons, then we can estimate their density from (23). This estimate provides an *upper limit* for the instanton density

$$\left(\frac{N}{V}\right) \leq \frac{1}{32\pi^2}\langle (G^a_{\mu\nu})^2\rangle \simeq 1\,{\rm fm}^{-4}. \tag{26}$$

A similar estimate can be obtained from the (pure gauge) topological susceptibility. The value of $\chi_{\rm top}$ in quenched QCD can be estimated from the Witten-Veneziano relation[26, 27]

$$\chi_{\rm top} = 2f_\pi^2(m_\eta^2 + m_{\eta'}^2 - 2m_K^2) = (180\,{\rm MeV})^4. \tag{27}$$

Using the result (25), we again get $(N/V) \simeq 1$ fm^{-4}.

The other important parameter characterizing the instanton ensemble is the typical instanton *size*. If the total tunneling rate can be calculated from the semi-classical 't Hooft formula, then we can estimate the critical size by determining the maximum size up to which the rate has to be integrated in order to reproduce the phenomenological instanton density

$$\int_0^{\rho_{\rm max}} d\rho\, n_{\rm scl}(\rho) = n_{\rm phen} \tag{28}$$

Using $n_{\rm phen} = 1$ fm^{-4}, Shifman et al. concluded that $\rho_{\rm max} \simeq 1$ fm. This is a very pessimistic result, because it implies that there are no individual instantons and that their action is not large, so the semi-classical approximation is useless.

However, if instanton interact, the situation may be different. The role of interactions can also be estimated using the value of the gluon condensate

$$dn = dn_{\rm scl}\left[1 + \frac{\pi^4\rho^4}{2g^4}\langle (G^a_{\mu\nu})^2\rangle + \ldots\right]. \tag{29}$$

Using the canonical value of the gluon condensate, we see that for $\rho > 0.2$ fm the interaction of instantons with vacuum fields (of whatever origin) is not negligible. Also, we observe that interactions lead to a tunneling rate that grows faster than the semi-classical rate. Based on this result, we[4] suggested that the typical instanton size is significantly smaller,

$$\rho_{\rm max} \sim 1/3\,{\rm fm}. \tag{30}$$

If the average instanton is indeed small, we obtain a completely different picture of the QCD vacuum:

1. Since the instanton size is significantly smaller than the typical separation R between instantons, $\rho/R \sim 1/3$, the vacuum is fairly dilute. The fraction of spacetime occupied by strong fields is only a few per cent.

2. The fields inside the instanton are very strong $G_{\mu\nu} \gg \Lambda^2$. This means that the semi-classical approximation is valid, and the typical action is large

$$S_0 = 8\pi^2/g^2(\rho) \sim 10 - 15 \gg 1. \tag{31}$$

   Higher order corrections are proportional to $1/S_0$ and presumably small.

3. Instantons retain their individuality and are not destroyed by interactions. From the dipole formula, one can estimate

$$|\delta S_{\rm int}| \sim (2-3) \ll S_0. \tag{32}$$

4. Nevertheless, interactions are important for the structure of the instanton ensemble, since

$$\exp|\delta S_{\rm int}| \sim 20 \gg 1. \tag{33}$$

   This implies that interactions have a significant effect on correlations among instantons, the instanton ensemble in QCD is not a dilute gas, but an interacting liquid.

Improved estimates of the instanton size can be obtained from phenomenological applications of instantons. The average instanton size determines the structure of chiral symmetry breaking, in particular the values of the quark condensate, the pion mass, its decay constant and its form factor. We will discuss these observables in more detail below.

The instanton liquid is "distilled" from the lattice

Instantons start emerging from the "fog" of quantum fluctuations, when lattice configurations were subjected to operations making the gauge field more smooth. The most popular one known as "cooling" rapidly kills the short-wavelength quantum noise and leads to a local minimum, a kind of classical content of the configuration. In Fig. 2 from[15] one can see how it works.

After counting the instantons, and transferring the resulting density in absolute units†, these authors have concluded‡ that the instanton density in *quenched* QCD is about 1.3-1.6 fm^{-3}.

The average size of an instanton[4] $\rho \sim 1/3$ fm has been confirmed qualitatively many years ago by[30], and now more quantitative measurements[15] give $\rho = .35$ fm. Furthermore, the *shape* of the instanton size distribution function, $d(\rho)$, was recently measured on the lattice[31] (for pure $SU(2)$ theory). Their results are compared in Fig. 3. The agreement is best for large instanton sizes and it is not good for small

†The units are fixed by the measurement of the ρ meson mass and demanding it to be equal to the experimental value.

‡Unfortunately, the cooling method has some systematic errors. If the simplest Wilson action is used, instantons gradually shrink and finally "drop through the lattice". More sophisticated actions prevent that and make lattice instantons stable. Another approach recently developed is called the "inverse blocking": it allows to recover instantons with a radius as small as $.8a$.

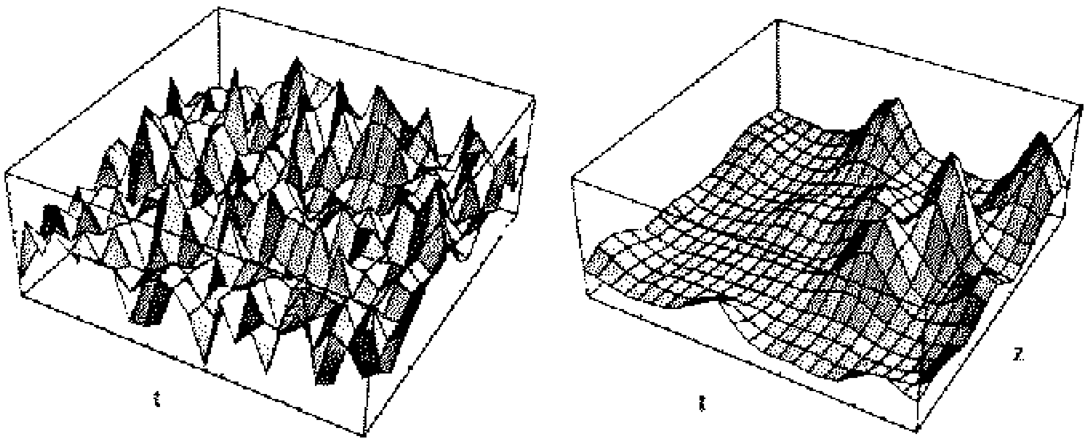

Figure 2. Sample of a gauge configuration before (left) and after (right) cooling. In the latter case instantons are clearly seen. The quantity shown is the action density, and its scale (not shown) is two orders of magnitude larger on the left figure.

ones[§]. That is of course exactly as expected: instantons with the radius $\rho \sim a$ "fall through the lattice" during "cooling". The main fact is a confirmation of a sharp maximum, with strong suppression of large-size[¶] instantons. The open points in Fig. 3 are the "instanton liquid" calculations[29].

Another striking news[15] came from the correlators calculated *after cooling* of lattice configurations (so to say, in the instanton liquid distilled from them). In spite of apparent loss of perturbative effects and (nearly complete) loss of confinement, the correlators stubbornly remained about the same. It is hardly possible to demonstrate more clearly that perturbative phenomena (the Coulomb and spin-spin forces) and confinement are not in fact so important for hadronic properties!

Zero Modes and the $U(1)_A$ anomaly

Instantons interpolate between different topological vacua in QCD. It is then natural to ask if the different vacua can be physically distinguished. This question is answered in the presence of light fermions, because the different vacua have different axial charge. This observation is the key element in understanding the mechanism of "anomalies". Anomalies first appeared in the context of perturbation theory[32, 33]. From the triangle diagram involving an external axial vector current one finds that the flavor singlet current which is conserved on the classical level develops an anomalous divergence on the quantum level

$$\partial_\mu j^5_\mu = \frac{N_f}{16\pi^2} G^a_{\mu\nu} \tilde{G}^a_{\mu\nu}. \tag{34}$$

This anomaly plays an important role in QCD, because it explains the absence of a ninth goldstone boson, the so-called $U(1)_A$ puzzle.

The mechanism of the anomaly is intimately connected with instantons. First, we recognize the integral of the rhs of (34) as $2N_f Q$, where Q is the topological charge. This means that in the background field of an instanton we expect axial charge conservation

[§]In passing, let us mention here one practical aspect of the studies of $d(\rho)$: its measurements at *small* $\rho < 0.2$ fm is potentially the source of by far the most accurate measurements of $\Lambda_{\rm QCD}$. As it is well known, here $d(\rho) \sim \Lambda^{b_0}_{\rm QCD}$: thus even relatively poor accuracy in its measurements leads to a $\Lambda_{\rm QCD}$ value with the accuracy better than measured today by other methods.

[¶]Note that unlike small ones, those are measured reliably.

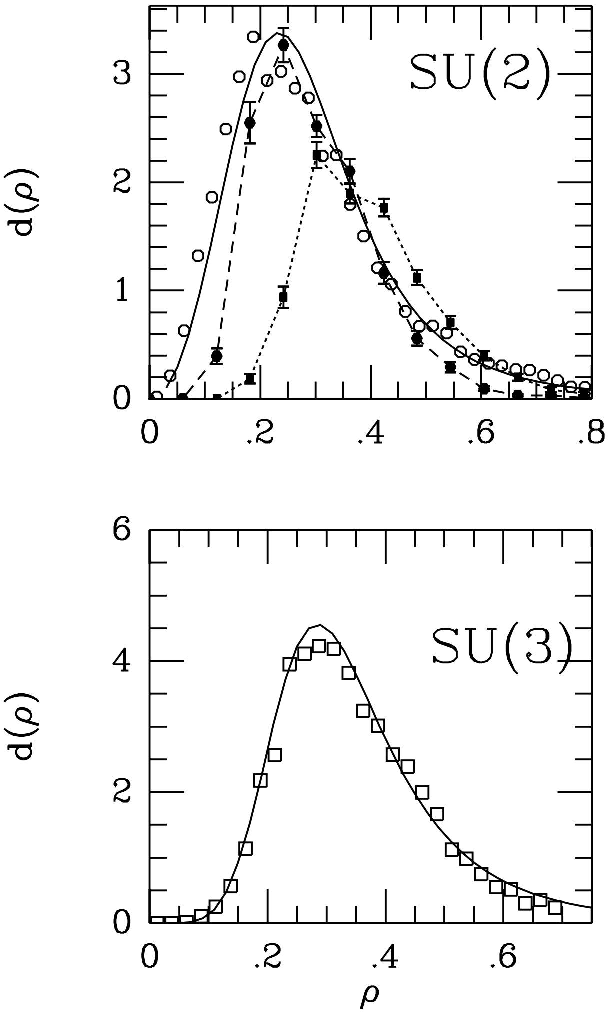

Figure 3. The instanton size distribution in gauge theories. The open points correspond to interacting instanton liquid", and the closed ones are lattice results by Michael and Spencer, $16^4, 4/g^2 = 2.4$ for squares and $24^4, 4/g^2 = 2.5$ for dots (the dotted and dashed lines just guide the eye). Solid curves correspond to the parameterization discussed in the text. Units are in "femtometers", defined for lattice data by the scalar glueball mass defined as $m_{0^+} = 1.7$ "GeV"; and by $1/\Lambda_{PV}$ for the instanton model.

to be violated by $2N_f$ units. The crucial property of instantons, originally discovered by 't Hooft, is that the Dirac operator has a zero mode $i\not{D}\psi_0(x) = 0$ in the instanton field. For an instanton in the singular gauge, the zero mode wave function is

$$\psi_0(x) = \frac{\rho}{\pi}\frac{1}{(x^2+\rho^2)^{3/2}}\frac{\gamma\cdot x}{\sqrt{x^2}}\frac{1+\gamma_5}{2}\phi \tag{35}$$

where $\phi^{\alpha m} = \epsilon^{\alpha m}/\sqrt{2}$ is a constant spinor, which couples the color index α to the spin index $m = 1, 2$. Note that the solution is left handed, $\gamma_5\psi_0 = -\psi_0$. Analogously, in the field of an anti-instanton there is a right handed zero mode.

We can now see how axial charge is violated during tunneling[34, 35]. For this purpose, let us consider the Dirac Hamiltonian $i\vec{\alpha}\cdot\vec{D}$ in the field of the instanton. The presence of a four dimensional normalizable zero mode implies that there is one left handed state that crosses from positive to negative energy during the tunneling event, while one right handed state crosses the other way. This can be seen as follows: In the adiabatic approximation, solutions of the Dirac equation are given by

$$\psi_i(\vec{x},t) = \psi_i(\vec{x},t=-\infty)\exp\left(-\int_{-\infty}^{t} dt'\,\epsilon(t')\right). \tag{36}$$

The only way we can have a four-dimensional normalizable wave function is if the energy ϵ is positive for $t\to\infty$ and negative for $t\to-\infty$. This explains how axial charge can be violated during tunneling. No fermion ever changes its chirality, all states simply move one level up or down. The axial charge comes, so to say, from the "bottom of the Dirac sea".

The effective interaction between quarks

Proceeding from pure glue theory to QCD with light quarks, one has to deal with the much more complicated problem of quark-induced interactions. Indeed, on the level of a single instanton we can not even understand the presence of instantons in full QCD. The reason is again related to the existence of zero modes. In the presence of light quarks, the tunneling rate is proportional to the fermion determinant, which is given by the product of the eigenvalues of the Dirac operator. This means that (as $m\to 0$) the fermion zero mode makes the tunneling amplitude vanish and individual instantons cannot exist!

During the tunneling event, the axial charge of the vacuum changes, so instantons have to be accompanied by flipping of the fermion chirality. Consider the fermion propagator in the instanton field

$$S(x,y) = \frac{\psi_0(x)\psi_0^+(y)}{im} + \sum_{\lambda\neq 0}\frac{\psi_\lambda(x)\psi_\lambda^+(y)}{\lambda+im} \tag{37}$$

where $i\not{D}\psi_\lambda = \lambda\psi_\lambda$. For N_f light quark flavors the instanton amplitude is proportional to m_f^N. Instead of the tunneling amplitude, let us calculate a $2N_f$-quark Green's function $\langle\prod_f \bar\psi_f(x_f)\Gamma\psi_f(y_f)\rangle$, containing one quark and antiquark of each flavor. Performing the contractions, the amplitude involves N_f fermion propagators (37), so that the zero mode contribution involves a factor m^{N_f} in the denominator.

The result can be written in terms of an effective Lagrangian[22]. It is a non-local $2N_f$-fermion interaction, where the quarks are emitted or absorbed in zero mode wave functions. The result simplifies if we take the long wavelength limit (in fact, the interaction is cut off at momenta $k>\rho^{-1}$) and average over the instanton position and color orientation. For $N_f=1$ the result is[36, 37]

$$\mathcal{L}_{N_f=1} = \int d\rho\, n_0(\rho)\left(m\rho - \frac{4}{3}\pi^2\rho^3\bar q_R q_L\right), \tag{38}$$

where $n_0(\rho)$ is the tunneling rate. Note that the zero mode contribution acts like a mass term. For $N_f=2$, the result is

$$\mathcal{L}_{N_f=2} = \int d\rho\, n_0(\rho)\Big[\prod_f\left(m\rho - \frac{4}{3}\pi^2\rho^3\bar q_{f,R}q_{f,L}\right) \tag{39}$$
$$+\frac{3}{32}\left(\frac{4}{3}\pi^2\rho^3\right)^2\left(\bar u_R\lambda^a u_L\bar d_R\lambda^a d_L - \bar u_R\sigma_{\mu\nu}\lambda^a u_L\bar d_R\sigma_{\mu\nu}\lambda^a d_L\right)\Big].$$

One can easily check that the interaction is $SU(2)\times SU(2)$ invariant, but $U(1)_A$ is explicitly broken.

INTERACTING INSTANTON LIQUID AND HADRONS

There is no place here to describe the interacting model: let me only mention that it includes the whole zero-mode part of the fermionic determinant, which means that the 't Hooft interaction is included to *all* orders. Methodically it is similar to usual statistical simulations. One new element[38] which was incorporated only recently is a trick which has allowed us to calculate the absolute value of the partition function: as a result the instanton density is now fixed from the standard condition of minimizing the free energy.

The interacting liquid is qualitatively different from the random one in several important aspects. It obeys known low energy theorems (see[38]), screens the topological charge and provides vanishing topological susceptibility[39], etc. Let me only comment that some improvement is definitely seen in vector-axial channels, and they are really dramatic in "repulsive" η, δ channels, in which RILM has produced unphysical negative correlators. One can see that indeed those are due to correlations between instantons and anti-instantons, induced by quark exchanges.

The calculated correlation functions

Correlation functions in the different instanton ensembles were calculated in[40, 8, 38] to which we refer the reader for more details. The results are shown in Figs. 4-5. The pion correlation functions in the different ensembles are qualitatively very similar. The differences are mostly due to different values of the quark condensate (and the physical quark mass) in the different ensembles. Using the Gell-Mann, Oaks, Renner relation, one can extrapolate the pion mass to the physical value of the quark masses. The results are consistent with the experimental value in the streamline ensemble (both

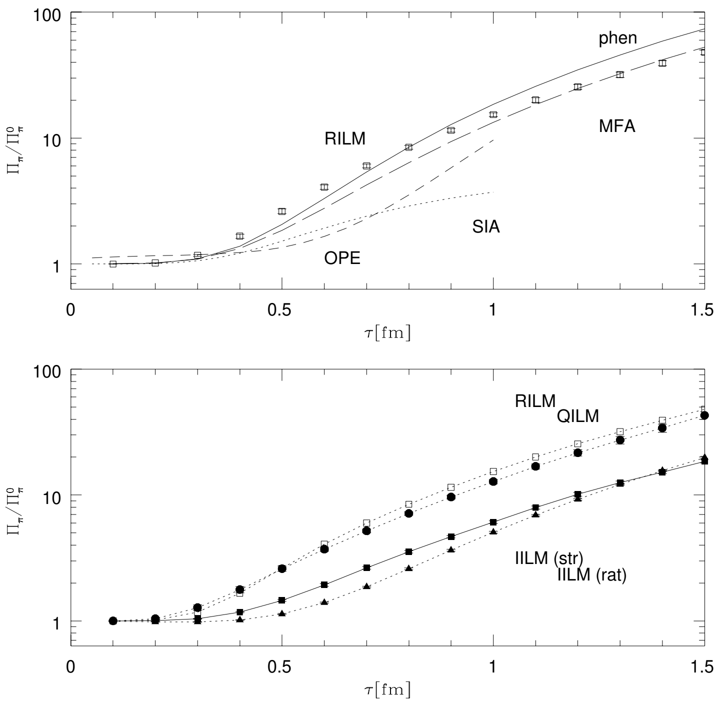

Figure 4. Pion correlation function in various approximations and instanton ensembles. In the top figure we show the phenomenological expectation (solid), the OPE (dashed), the single instanton (dash-dotted) and mean field approximations (dashed) as well as data in the random instanton ensemble. In the bottom figure we compare different instanton ensembles, random (open squares), quenched (circles) and interacting (streamline: solid squares, ratio ansatz solid triangles).

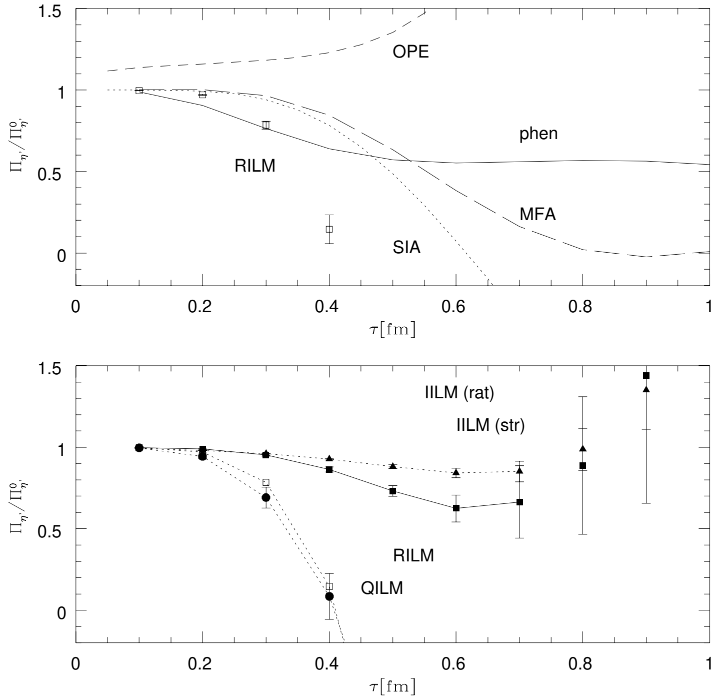

Figure 5. Eta prime meson correlation functions. The various curves and data sets are labeled as in Fig. 4.

quenched and unquenched), but clearly too small in the ratio ansatz ensemble. This is a reflection of the fact that the ratio ansatz ensemble is not sufficiently dilute.

In Fig. 6 we also show the results in the ρ channel. The ρ meson correlator is not affected by instanton zero modes to first order in the instanton density. The results in

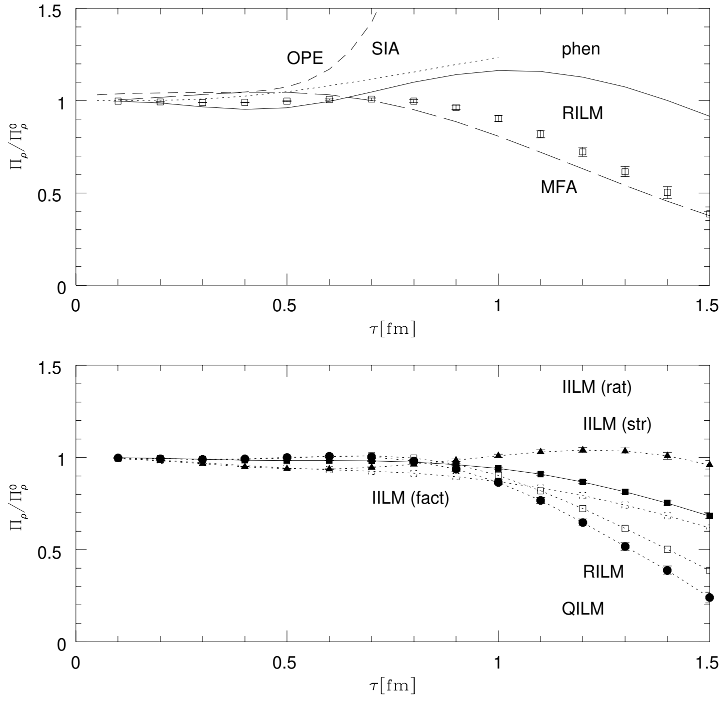

Figure 6. Rho meson correlation functions. The various curves and data sets are labeled as in Fig. 4. The dashed squares show the non-interacting part of the rho meson correlator in the interacting ensemble.

the different ensembles are fairly similar to each other and all fall somewhat short of the phenomenological result at intermediate distances $x \simeq 1$ fm. We have determine the ρ meson mass and coupling constant from a fit. The ρ meson mass is somewhat too heavy in the random and quenched ensembles, but in very good agreement with the experimental value $m_\rho = 770$ MeV in the interacting ensemble.

Since there are no interactions in the ρ meson channel in the RPA, it is important to study whether the instanton model provides any binding at all. In the instanton model, there is no confinement, and m_ρ is close to the two (constituent) quark threshold. In QCD, the ρ meson is also not a true bound state, but a resonance in the 2π continuum. In order to determine whether the continuum contribution in the instanton model is predominantly 2π or 2 quark would require the determination of the corresponding three point functions (which has not been done yet). Instead, we will compare the full correlation function with the non-interacting one, where we use the average (constituent quark) propagator determined in the same ensemble (Fig. 6). As explained above, this comparison provides a measure of the strength of interaction. We observe that there is an attractive interaction generated in the interacting liquid. The interaction is due to correlated instanton-anti-instanton pairs. This is consistent with the fact that the interaction is considerably smaller in the random ensemble. In the random model, the strength of the interaction grows as the ensemble becomes more dense. However, the interaction in the full ensemble is significantly larger than in the random model at the same diluteness. Therefore, most of the interaction comes from dynamically generated pairs.

The situation is drastically different in the η' channel. Among the ~ 40 correlation functions calculated in the random ensemble, only the η' (and the isovector-scalar δ discussed in the next section) are completely unacceptable: The correlation function decreases very rapidly and becomes negative at $x \sim 0.4$ fm. This behavior is incompatible with a normal spectral representation. The interaction in the random ensemble is too repulsive, and the model "over-explains" the $U(1)_A$ anomaly.

The results in the unquenched ensembles (closed and open points) significantly improve the situation. This is related to dynamical correlations between instantons and anti-instantons (topological charge screening). The single instanton contribution is repulsive, but the contribution from pairs is attractive[41]. Only if correlations among instantons and anti-instantons are sufficiently strong, the correlators are prevented from becoming negative. Quantitatively, the δ and $\eta_{\rm ns}$ masses in the streamline ensemble are still too heavy as compared to their experimental values. In the ratio ansatz, on the other hand, the correlation functions even show an enhancement at distances on the order of 1 fm, and the fitted masses are too light. This shows that the η' channel is very sensitive to the strength of correlations among instantons.

In summary, pion properties are mostly sensitive to global properties of the instanton ensemble, in particular its diluteness. Good phenomenology demands $\bar\rho^4 n \simeq 0.03$, as originally suggested in[42]. The properties of the ρ meson are essentially independent of the diluteness, but show sensitivity to $\bar{I}I$ correlations. These correlations become crucial in the η' channel.

After discussing the π, ρ, η' in some detail we only briefly comment on other correlation functions. The remaining scalar states are the isoscalar σ and the isovector δ (the a_0, f_0 in modern PDG notations). The sigma correlator receives a disconnected contribution, which at large distance is dominated by the quark condensate. In order to determine the ground state in this channel, the constant contribution has to be subtracted, which makes it difficult to obtain reliable results. Nevertheless, we find that the instanton liquid favors a (presumably broad) resonance around 500-600 MeV.

The isovector channel is in many ways similar to the η'. In the random ensemble, the interaction is too repulsive and the correlator becomes unphysical. This problem is solved in the interacting ensemble, but the δ is still very heavy, $m_\delta > 1$ GeV.

The remaining non-strange vectors are the a_1, ω and f_1. The a_1 mixes with the pion, which allows a determination of the pion decay constant f_π (as does a direct measurement of the $\pi - a_1$ mixing correlator). In the instanton liquid, disconnected contributions in the vector channels are small. This is consistent with the fact that the ρ, ω and a_1, f_1 are almost degenerate.

Finally, we can also include strange quarks. $SU(3)$ flavor breaking in the 't Hooft interaction nicely accounts for the masses of the K and the η. More difficult is a correct description of $\eta - \eta'$ mixing, which can only be achieved in the full ensemble. The random ensemble also has a problem with the mass splittings among the vectors ρ, K^*, ϕ. This is related to the fact that flavor symmetry breaking in the random ensemble is so strong that the strange and non-strange constituent quark masses are essentially the same. This problem is improved (but not fully solved) in the interacting ensemble.

Baryonic correlation functions

After discussing quark-antiquark systems in the last section, we now proceed to three quark (baryon) channels. As emphasized in[43], existence of a strongly attractive interaction in the pseudoscalar quark-antiquark (pion) channel also implies an attractive interaction in the scalar quark-quark (diquark) channel. This interaction is phenomenologically very desirable, because it immediately explains why the nucleon and lambda are light, while the delta and sigma are heavy.

The proton current can be constructed by coupling a d-quark to a uu-diquark. The diquark has the structure $\epsilon_{abc} u_b C\Gamma u_c$ which requires that the matrix $C\Gamma$ is symmetric. This condition is satisfied for the V and T gamma matrix structures. The two possible currents (with no derivatives and the minimum number of quark fields) with positive parity and spin 1/2 are given by[44]

$$\eta_1 = \epsilon_{abc}(u^a C\gamma_\mu u^b)\gamma_5\gamma_\mu d^c, \qquad \eta_2 = \epsilon_{abc}(u^a C\sigma_{\mu\nu} u^b)\gamma_5\sigma_{\mu\nu} d^c. \tag{40}$$

It is sometimes useful to rewrite these currents in terms of scalar and pseudoscalar diquarks

$$\eta_{1,2} = (2,4)\left\{\epsilon_{abc}(u^a C d^b)\gamma_5 u^c \mp \epsilon_{abc}(u^a C\gamma_5 d^b) u^c\right\}. \tag{41}$$

Nucleon correlation functions are defined by $\Pi^N_{\alpha\beta}(x) = \langle \eta_\alpha(0)\bar\eta_\beta(x)\rangle$, where α, β are the Dirac indices of the nucleon currents. In total, there are six different nucleon correlators: the diagonal $\eta_1\bar\eta_1$, $\eta_2\bar\eta_2$ and off-diagonal $\eta_1\bar\eta_2$ correlators, each contracted with either the identity or $\gamma\cdot x$. Let us focus on the first two of these correlation functions (for more detail, see[8] and references therein). The OPE predicts[45])

$$\frac{\Pi^N_1}{\Pi^{N0}_2} = \frac{\pi^2}{12}|\langle\bar q q\rangle|\tau^3, \tag{42}$$

$$\frac{\Pi^N_2}{\Pi^{N0}_2} = 1 + \frac{\pi^2}{192}\left\langle\frac{\alpha}{\pi}G^2\right\rangle\tau^4 + \frac{\pi^4}{72}|\langle\bar q q\rangle|^2\tau^6. \tag{43}$$

The vector components of the diagonal correlators receive perturbative quark-loop contributions, which are dominant at small distances. The scalar components of the diagonal correlators as well as the off-diagonal correlation functions are sensitive to chiral symmetry breaking, and the OPE starts at order $\langle\bar{q}q\rangle$ or higher. Single instanton corrections to the correlation functions were calculated in[46, 47]*. Instantons introduce additional, regular, contributions in the scalar channel and violate the factorization assumption used for the four-quark condensate in the vector channel. Similar to the pion case, both of these effects increase the amount of attraction already seen in the OPE. As shown in[47], they also help to improve the stability of the QCD sum rule predictions for the nucleon mass.

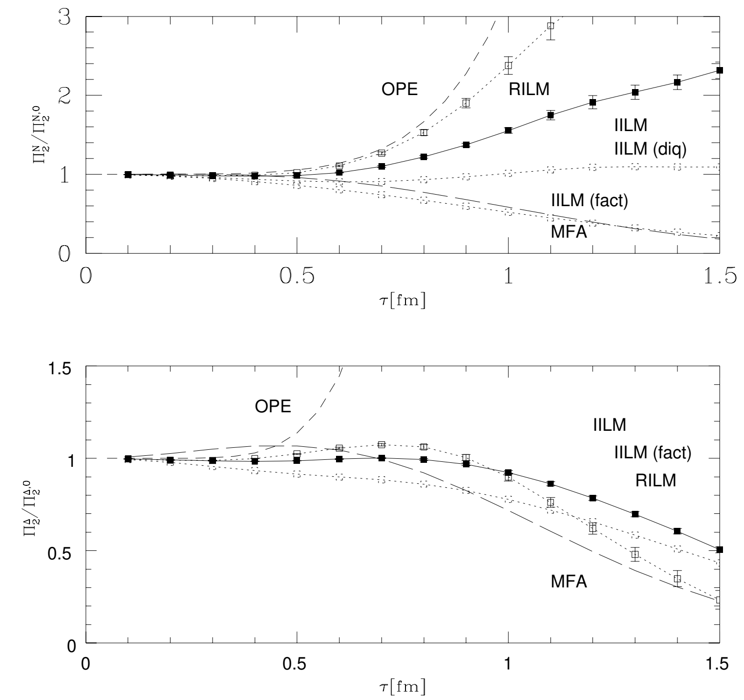

Figure 7. Nucleon and delta correlation functions Π_2^N and Π_2^Δ. Curves labeled as in Figs. 4-6.

The correlation function Π_2^N in the interacting ensemble is shown in Fig. 7. There is a significant enhancement over the perturbative contribution which is nicely described in terms of the nucleon contribution. Numerically, we find† $m_N = 1.019$ GeV. In the random ensemble, we have measured the nucleon mass at smaller quark masses and found $m_N = 0.96 \pm 0.03$ GeV. The nucleon mass is fairly insensitive to the instanton ensemble. However, the strength of the correlation function depends on the instanton ensemble. This is reflected by the value of the nucleon coupling constant, which is smaller in the IILM.

The fitted value of the threshold is $E_0 \simeq 1.8$ GeV, indicating that there is little strength in the (unphysical) three quark continuum. The fact that nucleon is bound can also be demonstrated by comparing the full nucleon correlation function with that of three non-interacting quarks (the cube of the average propagator, see Fig. 7). The full correlator is significantly larger than the non-interacting one, indicating the presence of a strongly attractive interaction. At least some of this interaction certainly comes from the attractive scalar diquark correlator which is part of the nucleon correlation function. This raises the question whether the nucleon (in our model) is a strongly bound diquark very loosely coupled to a third quark. In order to check this, we can rewrite the NN correlation functions using (41). Treating the nucleon as a non-interacting quark-

*The latter paper corrects some mistakes in the original work by Dorokhov and Kochelev.
†Note that this value corresponds to a relatively large current quark mass $m = 30$ MeV.

diquark system, we have

$$\Pi_2^N(\tau) = 4S_V(\tau)\left(\Pi_{\rm sd}(\tau) + \Pi_{\rm pd}(\tau)\right) + 96 S_V(\tau) S_S^2(\tau), \tag{44}$$

where $\Pi_{\rm sd,pd}(\tau)$ are the correlation functions of the scalar $j^a_{\rm sd} = \epsilon^{abc}(u^a C\gamma_5 d^b)$ and pseudoscalar diquark $j^a_{\rm pd} = \epsilon^{abc}(u^a C d^b)$ currents. From Fig. 7 we observe that the quark-diquark model explains some of the attraction seen in Π_2^N, but falls short of the numerical results. This means that while diquarks may play some role in making the nucleon bound, there are substantial interactions in the quark-diquark system.

In[8] we studied all six nucleon correlation functions. We showed that all correlation functions can be described with the same nucleon mass and coupling constants. This description is particularly good for the $\Pi_{1,2}^N$ and $\Pi_{4,5}^N$ correlators, but misses some of the contributions at intermediate distances in the $\Pi_{3,6}^N$ channels. This might be an indication that in these channels contributions from higher resonances are important.

Delta correlation functions

In the case of the Δ resonance, there exists only one independent current, given (for the Δ^{++}) by

$$\eta_\mu^\Delta = \epsilon_{abc}(u^a C\gamma_\mu u^b)u^c. \tag{45}$$

However, the spin structure of the correlator $\Pi^\Delta_{\mu\nu;\alpha\beta}(x) = \langle \eta^\Delta_{\mu\alpha}(0)\bar\eta^\Delta_{\nu\beta}(x)\rangle$ is much richer. In general, there are ten independent tensor structures, but the Rarita-Schwinger constraint $\gamma^\mu\eta^\Delta_\mu = 0$ reduces this number to four.

The mass of the delta resonance is too large in the random model, but closer to experiment in the unquenched ensemble. Note that similar to the nucleon, part of this discrepancy is due to the value of the current mass. Nevertheless, the delta-nucleon mass splitting in the unquenched ensemble is $m_\Delta - m_N = 409$ MeV, still too large as compared to the experimental value 297 MeV. Similar to the ρ meson, there is no binding in the Δ channel on the level of the mean field approximation. Comparing the full correlation function with the non-interacting one (see Fig. 7) we find substantial attraction between the quarks. Again, it would be important to show that the continuum is dominated by $N\pi$ rather than the three quark threshold. In addition to the results presented here, heavy-light baryons were studied in[8, 9].

GLUEBALLS AND INSTANTONS

One of the most interesting problems in hadronic spectroscopy is the question how the glueball states look like. A number of "glueball candidates" have been experimentally observed, but none was unambiguously identified. Lattice simulations provide important qualitative insights, and (although large-scale numerical efforts are still necessary) a few statements appear to be firmly established: (i) The lightest glueball is the scalar, with a mass in the 1.5-1.7 GeV range. (ii) The tensor glueball is significantly heavier $m_{2^{++}}/m_{0^{++}} \simeq 1.4$, with the pseudoscalar one heavier still $m_{0^{-+}}/m_{0^{++}} = 1.5$-$1.8$. (iii) The scalar has a much smaller size than other glueballs. This is seen both from the magnitude of finite size effects[48] and directly from measurements of the wave functions[49, 50]. The size of the scalar glueball (defined through the exponential decay of the wave function) is $r_{0^{++}} \simeq 0.2$ fm, while[50] $r_{2^{++}} \simeq 0.8$ fm*.

*For comparison, a similar measurement for the π and ρ mesons gives[50] 0.32 fm and 0.45 fm, indicating that spin-dependent forces between gluons are stronger than between quarks.

Instantons are expected to give a large contribution to glueball correlation functions because of their very strong classical gluonic field. Roughly speaking, they contribute proportionally to the square of their action $S_0 = 8\pi^2/g^2(\rho) \sim 10-15$, so enhancement is about 2 orders of magnitude.

Gluonic currents with the quantum numbers of the lowest glueball states are the field strength squared (0^{++}), the topological charge density (0^{-+}), and the energy momentum tensors (2^{++}): For the scalar channel a *single instanton* contribution is attractive, for the pseudoscalar channel it is repulsive, and for the tensor channel there is no classical contribution since the stress tensor of the self-dual field of an instanton is zero. To study this question in more detail, and in order to determine the effect of light quarks on the glueball correlation functions we have calculated glueball correlation functions numerically in the different instanton ensembles[3]. As usual we parameterize the glueball correlators using a pole plus continuum model for the spectral function. The scalar glueball mass is roughly $m_{0^{++}} = 1.5$ GeV with deviations of up to 0.25 GeV depending on the underlying ensemble. Given the uncertainties in the mass determination (the scalar correlator requires a subtraction), it is not clear whether these differences are significant. The coupling constant is almost independent of the ensemble $\lambda_{0^{++}} = 16 \pm 2$ GeV^3[†]. This large coupling, as well as direct study of the wave function have lead to a very small size for a scalar glueball, about .2 fm.

In the pseudoscalar case the classical and one-loop contributions have opposite signs. At distances where they tend to cancel each other our approximation (which neglects the interference between the two) becomes questionable. However, the rapid downturn directly translates into the position of the perturbative threshold, for which we find $\sqrt{s_0} \simeq 2.4$ GeV in the quenched theory. We see no clear evidence for a pseudoscalar glueball state below the continuum threshold. In the unquenched theory we observe the η' signal with $m_{\eta'} \approx 800$ MeV and $\lambda_{\eta'} \sim 7.0$ GeV^3. Using the anomaly equation, this corresponds to $f_{\eta'} = 200$ MeV.

The next step is to calculate the glueball decay widths: work is in progress.

INSTANTONS AND CHARM

We have discussed in the introduction a scale of 1 GeV which is related to the field strength at the center of a typical instanton. Note that it is not very small compared to the charm quark mass $m_c^2 \approx 2$ GeV^2, and thus one may expect some significant polarization of the charm quark vacuum. It means that hadrons made of light quarks may in fact have some instanton-induced "intrinsic charm", especially those which are most closely related to instantons.

It was found recently[65] that this seems to be the case for η' meson. It started when the CLEO collaboration reported[64] measurements of inclusive and exclusive production of the η' in B-decays:

$$Br(B \to \eta' + X\ ; 2.2\ GeV < E_{\eta'} < 2.7\ GeV) = (7.5 \pm 1.5 \pm 1.1) \cdot 10^{-4}\ , \tag{46}$$

$$Br(B \to \eta' + K) = (7.8^{+2.7}_{-2.2} \pm 1.0) \cdot 10^{-5}\ . \tag{47}$$

Simple estimates[66] show that these data are in severe contradiction with the standard b-quark decay into light quarks: Cabbibo suppression V_{ub} leads to decay rates two orders

[†]This number is significantly larger than the result of QCD sum rule calculations that do not enforce the low energy theorem[51, 52].

of magnitude smaller than the data (both inclusive and exclusive ones). An alternative mechanism, suggested in[66], is based on the Cabbibo favored $b \to c\bar{c}s$ process, followed by a transition of virtual $\bar{c}c$ into the η'. The latter transition may be possible, provided there exists a large intrinsic charm component of the η'. Its quantitative measure can be expressed through the matrix element

$$\langle 0|\bar{c}\gamma_\mu\gamma_5 c|\eta'(q)\rangle \equiv i f_{\eta'}^{(c)} q_\mu \ . \tag{48}$$

and one needs $f_{\eta'}^{(c)} \approx 140$ MeV in order to explain the CLEO data, see[66]. This value is surprisingly large, being only a few times smaller than the analogously normalized residue $\langle 0|\bar{c}\gamma_\mu\gamma_5 c|\eta_c(q)\rangle = i f_{\eta_c} q_\mu$ with $f_{\eta_c} \simeq 400$ MeV known experimentally from the $\eta_c \to \gamma\gamma$ decay. It is also comparable to a similarly defined coupling of η' to the axial current of light quarks: note however that instantons in fact lead to *repulsive* interactions between them, and thus the light quark wave function of η' should be depleted at the origin.

Because the c-quark is heavy, it may only exist in the η' through a virtual loop, and its contribution can be evaluated in terms of gluonic fields. Taking the divergence of the axial current in Eq.(48) one gets

$$f_{\eta'}^{(c)} = \frac{1}{m_{\eta'}^2}\langle 0|2m_c\bar{c}i\gamma_5 c + \frac{\alpha_s}{4\pi}G_{\mu\nu}\tilde{G}_{\mu\nu}|\eta'\rangle \tag{49}$$

which can be further simplified by the operator product expansion in inverse powers of the $c-$quark mass

$$2m_c\bar{c}i\gamma_5 c = -\frac{\alpha_s}{4\pi}G_{\mu\nu}\tilde{G}_{\mu\nu} - \frac{1}{16\pi^2 m_c^2}g^3 f^{abc}G^a_{\mu\nu}\tilde{G}^b_{\nu\alpha}G^c_{\alpha\mu} + \mathcal{O}(G^4/m_c^4) \tag{50}$$

(see the appendix in[66] for a detailed derivation of this result. Further terms in the expansion (50) are neglected in what follows.) Thus the problem is reduced to the matrix element of a particular dimension six pseudo-scalar gluonic operator:

$$f_{\eta'}^{(c)} = -\frac{1}{16\pi^2 m_{\eta'}^2}\frac{1}{m_c^2}\langle 0|g^3 f^{abc}G^a_{\mu\nu}\tilde{G}^b_{\nu\alpha}G^c_{\alpha\mu}|\eta'\rangle \ . \tag{51}$$

The calculation is based on numerical evaluation of the following two-point Euclidean correlation functions

$$K_{22}(x) = \langle 0|g^2 G^a_{\mu\nu}\tilde{G^a_{\mu\nu}}(x) g^2 G^a_{\mu\nu}\tilde{G^a_{\mu\nu}}(0)|0\rangle \tag{52}$$

$$K_{23}(x) = \langle 0|g^2 G^a_{\mu\nu}\tilde{G^a_{\mu\nu}}(x) g^3 f^{abc}G^a_{\mu\nu}\tilde{G}^b_{\nu\lambda}G^c_{\lambda\mu}(0)|0\rangle \tag{53}$$

$$K_{33}(x) = \langle 0|g^3 f^{abc}G^a_{\mu\nu}\tilde{G}^b_{\nu\lambda}G^c_{\lambda\mu}(x) \ \ g^3 f^{abc}G^a_{\mu\nu}\tilde{G}^b_{\nu\lambda}G^c_{\lambda\mu}(0)|0\rangle \tag{54}$$

Studies of $K_{22}(x)$ have been made previously[3], where it was demonstrated that in the "unquenched" ensemble of instantons with dynamical quarks the non-perturbative part changes sign at distances $x > 0.6$ fm, displaying a "Debye cloud" of compensating topological charge. It is identified with the η' contribution, and leads to an estimate

$$\langle 0|g^2 G^a_{\mu\nu}\tilde{G}^a_{\mu\nu}|\eta'\rangle = \frac{16\pi^2}{\sqrt{3}} f_{\eta'} m_{\eta'}^2 \approx 7 \ \ \mathrm{GeV}^3 \tag{55}$$

which agrees reasonably well with other estimates in the literature. In this formula we have expressed matrix element (55) in terms of the standard parameter $f_{\eta'} \approx 85$ MeV which is defined as follows

$$\langle 0|\frac{1}{\sqrt{3}}\sum_{i=u,d,s}\bar{q}_i\gamma_\mu\gamma_5 q_i|\eta'\rangle = i f_{\eta'} q_\mu .$$

Using an anomaly in the chiral limit, $m_u = m_d = m_s = 0$, we arrive at (55).

We have calculated by numerical simulation the correlators mentioned. At small x purely perturbative gluons (e.g. $K_{22}^{\rm pert}(x) = 384 g^4/\pi^4 x^8$) dominate, while the non-perturbative fields can be included via the operator product expansion. At large x we will argue below that (at least with dynamical quarks) the non-perturbative fields dominate.

The quantity $f_{\eta'}^{(c)}$ (51) can be obtained from the correlation functions (52, 53, 54):

$$|\frac{f_{\eta'}^{(c)}\sqrt{3}m_c^2}{f_{\eta'}}| = |\frac{K_{23}(x\to\infty)}{K_{22}(x\to\infty)}| = \sqrt{\frac{K_{33}(x\to\infty)}{K_{22}(x\to\infty)}} \tag{56}$$

It is expected that at large distances the contribution to two other correlators would also be dominated by the non-perturbative field of the instantons. If so, one has a simple estimate for the ratio of matrix elements

$$|\frac{\langle 0|g^3 f^{abc} G^a_{\mu\nu}\tilde{G}^b_{\nu\alpha}G^c_{\alpha\mu}|\eta'\rangle}{\langle 0|g^2 G^a_{\mu\nu}\tilde{G}^a_{\mu\nu}|\eta'\rangle}| = \frac{12}{5}\langle\frac{1}{\rho^2}\rangle \approx (1 \sim 1.5) GeV^2 \tag{57}$$

The two numbers given here correspond to averaging over instanton size distribution for two variants of the instanton-anti-instanton interaction, the so-called "streamline" and "ratio-ansatz" ones, and indicate the systematics involved. The latter (giving smaller average size and the larger number above) should be considered preferable, because it better agrees with the size distribution directly obtained from lattice gauge field configurations, see the discussion in[38].

In our measurements of K_{23}, K_{33} both ratios entering (56) were found to stabilize at large enough $x > 0.8$ fm at the *same* numerical value. We take it as an indication that the η' contribution does in fact dominate, although we were not able to see that all correlators fall off with the right mass. The numerical value of the ratios is about $(1.5 \sim 2.2)$ GeV^2, for the two ensembles mentioned. These numbers are somewhat larger than in (57) because the second operator in the correlator makes it more biased towards smaller instantons.

Proceeding to the final result, we have to consider QCD radiative corrections. The experimental number mentioned above is defined at the scale $\mu_1^2 \approx m_c^2$, which is different from that obtained in the instanton calculation. In the latter case the charge and fields are normalized at $\mu_2^2 \approx gG$ where G is the typical gauge field at the points which contribute most to the correlators. This concludes our derivation of the parameter

$$|\frac{f_{\eta'}^{(c)}}{f_{\eta'}}| \simeq (0.85 \sim 1.22), \tag{58}$$

where the second value is preferable, see above.

The next logical question to ask is whether the connection between strong instanton fields and charm leads to phenomena unrelated to η'. One intriguing direction to study is η_c hadronic decays: their deviations from a simple perturbative pattern (which works well for J/ψ) are well known, see e.g.[67]. Let us also mention the recent intriguing observation by Bjorken[68] that its three leading hadronic decay channels ($\eta'\pi\pi, \eta\pi\pi, KK\pi$) fit well to a pattern following from the instanton-induced 't Hooft effective Lagrangian.

Another question is whether the "intrinsic charm" (see e.g.[69]) of other hadrons is due to the same mechanism. Especially close to the problem considered is charm contribution to the spin of the nucleon. The relevant matrix element is that of the charm axial current, as above,

$$\langle N|\bar{c}\gamma_\mu\gamma_5 c|N\rangle = g_A^{(c)}\bar{N}\gamma_\mu\gamma_5 N \tag{59}$$

and it could be generated, e.g., by the η' "cloud" of the nucleon. Assuming now the η' dominance in this matrix element one could get the following Goldberger-Treiman type relation $g_A^{(c)} = \frac{1}{2M_N} g_{\eta' NN} f_{\eta'}^{(c)}$. Although the value of $g_{\eta' NN}$ is unknown, and its phenomenological estimates vary significantly $g_{\eta' NN} = 3-7$, one gets from this estimate a surprisingly large contribution

$$\langle N|\bar{c}\gamma_\mu\gamma_5 c|N\rangle = (0.2 \sim 0.5)\bar{N}\gamma_\mu\gamma_5 N \tag{60}$$

comparable to the *sum* (but not each term!) of the light u, d, s quarks. Calculation of $g_A^{(c)}$ and $g_{\eta' NN}$ in the instanton model are in progress: their lattice determination would be more than welcomed. Ultimately, the contribution of the charmed quarks in polarized deep-inelastic scattering may be tested experimentally, by tagging the charmed quark jets (e.g. by the COMPASS experiment at CERN).

In summary: it is by now widely known that the Zweig rule is badly broken in all scalar/pseudoscalar channels, and that the (rather large) mass of the η' is in fact due to light-quark-gluon mixing. Furthermore, these phenomena are generally attributed to instantons. We have found that similar phenomena for larger-dimension (multi-gluon) operators are much stronger. The reason for that is the inhomogeneous vacuum, with a very strong field inside small-size instantons. We have found a very significant fraction of charm in η'. Perhaps the same mechanism may help to solve other puzzles, especially related with η_c decays and DIS on the polarized nucleon.

THE CHIRAL PHASE TRANSITIONS

High temperature QCD

Let me first remind that non-zero T is incorporated in quantum field theory in a very simple way: the Euclidean time τ is limited by a period $1/T$, the so called Matsubara time. The instanton solution with periodic boundary conditions, called caloron, is analytically known.

$$A_\mu^a = \overline{\eta}_{\mu\nu}^a \Pi(x)\partial_\nu \Pi^{-1}(x) \tag{61}$$

where

$$\Pi(x) = 1 + \frac{\pi\rho^2}{\beta r}\frac{\sinh(2\pi r/\beta)}{\cosh(2\pi r/\beta) - \cos(2\pi\tau/\beta)} \tag{62}$$

Fermions should be *anti*−periodic, and the corresponding zero mode can also be found.

$$\psi_i^a = \frac{1}{2\sqrt{2}\pi\rho}\sqrt{\Pi(x)}\partial_\mu\left(\frac{\Phi(x)}{\Pi(x)}\right)\left(\frac{1-\gamma_5}{2}\gamma_\mu\right)_{ij}\epsilon_{aj}\,, \tag{63}$$

where $\Phi(x) = (\Pi(x) - 1)\cos(\pi\tau/\beta)/\cosh(\pi r/\beta)$. Note that the zero-mode wave function shows exponential decay $\exp(-\pi r T)$ in the spatial direction, but oscillates in τ.

So if instantons are like atoms with the quark zero mode as a wave function, finite T compresses their special extension and enhances the temporal one. (It looks like atoms in a very strong magnetic field.) That radically change their interactions, which are only strong if instantons are interacting along the time direction. In particular, a pair of such type can be formed, connected to themselves by periodicity.

The main finding in IILM at finite T is that the chiral phase transition is actually driven by a *rearrangement*[53, 41, 38] of the ensemble into a set of instanton anti-instanton "molecules"*. Recently the details of this mechanism were significantly clarified, both by numerical simulations[38] and analytic studies[54].

Let me start with some analytic arguments first. It was shown by Balitsky and Young[55] that in quantum mechanics coupled to fermions (in which the vacuum also is made of $\bar{I}I$ molecules) one can take the integral over the $\bar{I}I$ separation R by the saddle point method. Apart of the contribution from $R = 0$ (the perturbative saddle point) they have also found the non-perturbative contribution from large R. Unfortunately it is complex, unless the parameters are tuned so that the model is supersymmetric†. However, at *sufficiently high* T the non-perturbative saddle point becomes real again. It corresponds to a configuration in which the centers are at the same spatial point, but separated by half a Matsubara box in time $\Delta\tau = 1/(2T)$, the most symmetric orientation of the instanton anti-instanton pair on the Matsubara torus. The effect is largest when the molecule exactly fits onto the torus, i.e. $4\rho \simeq 1/T$. Using the standard size $\rho \simeq 0.33$ fm, one gets $T \simeq 150$ MeV, close to the transition temperature.

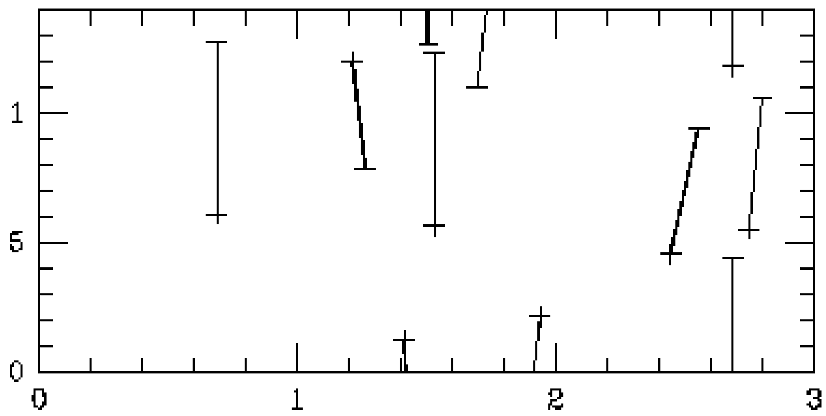

Figure 8. Typical instanton configurations for a temperature $T = 158$ MeV. The plot shows projection of a four dimensional box, $(3\Lambda^{-1})^3 \times T^{-1}$, into the 3-4 ($z$ axes-imaginary time) plane. Instanton and anti-instanton positions are indicated by $+$ and $-$ symbols. The lines correspond to the strongest fermionic "bonds".

In a series of recent numerical simulations[3] it was found that this transition indeed goes as expected, see Fig. 8, where molecules are clearly seen. Furthermore, many thermodynamic parameters, the spectra of the Dirac operator, the evolution of the quark condensate and susceptibilities were calculated[38, 54], with results surprisingly consistent with available lattice data.

*Note a similarity to the Kosterlitz-Thouless transition in the $O(2)$ spin model in two dimensions: again one has paired topological objects, vortices in one phase and random liquid in another. The high and low-temperature phase change places, though.

†In this case one can see that the answer they got is in fact correct.

The effect of molecules on the effective interaction between quarks at high temperature can be described by the effective Lagrangian

$$\mathcal{L}_{\mathrm{mol\,sym}} = G\left\{\frac{2}{N_c^2}\left[(\bar\psi\tau^a\psi)^2-(\bar\psi\tau^a\gamma_5\psi)^2\right]\right. \\ \left. -\frac{1}{2N_c^2}\left[(\bar\psi\tau^a\gamma_\mu\psi)^2+(\bar\psi\tau^a\gamma_\mu\gamma_5\psi)^2\right]+\frac{2}{N_c^2}(\bar\psi\gamma_\mu\gamma_5\psi)^2\right\}+\cdots, \tag{64}$$

with the coupling constant

$$G=\int d\rho_1 d\rho_2\,\frac{n(\rho_1,\rho_2)}{8T_{\bar II}^2}(2\pi\rho_1)^2(2\pi\rho_2)^2\,. \tag{65}$$

Here, $n(\rho_1,\rho_2)$ is the tunneling probability for the $\bar II$ pair and $T_{\bar II}$ is the corresponding overlap matrix element. τ^a is a four-vector with components $(\vec\tau,1)$.

Completely unexpected results were found in simulations, suggesting that some hadronic states (especially pions and its chiral partner sigma) survive the phase transition as a bound (but not-Goldstone) state. The interaction described above should be responsible for that.

High density QCD

Zero (or low) temperature and high density (or chemical potential μ) is another area in which one expects a phase transition in which chiral symmetry gets restored and quarks are "liberated". We know that normal nuclei consist of what is called nuclear matter, it has a baryon density of about $n_o \approx .16\ \mathrm{fm}^{-3}$, and is dilute enough to consist of individual nucleons. With the appearance of QCD it became apparent in the 70's that very high density matter should be more or less an ideal fermi gas of quarks. A very important feature in this case is Debye screening of color fields, and thus it is referred to as the quark plasma phase. Among other things, this screening cuts off large size instantons[4]

$$dn(\rho,\mu)\approx dn(\rho,\mu=0)\exp(-N_f\rho^2\mu^2) \tag{66}$$

in the same way as the high-temperature quark-gluon plasma does. In general, the properties of high-density quark plasma are rather well understood. However, very little is known about the transition from nuclear matter to the quark plasma. It may proceed via a number of intermediate phases, and many are discussed in literature.

In this subsection we study what can be learned about this transition using the instanton-based approach. One particular instanton-induced effect in vacuum is formation of specific correlations between two quarks, or *diquarks*. It was shown in many phenomenological papers that correlations of such kind seem to exist inside the nucleons, see the recent review[71].

In relation with this, it is very instructive to consider QCD with *two* colors. Discussion of the large-N_c limit of QCD is well known and is now part of text books. We remind only that in this limit the baryons should become very heavy $M_{baryons}\sim N_c^1$, as compared to mesons $M_{mesons}\sim N_c^0$, and all quarks should sit in the same lowest state in a semi-classical common potential well. Quite the opposite picture is the case for $N_c=2$. In the massless case an additional Pauli-Gursey symmetry (PGSY) exists[72], which incorporates mixing of quarks with anti-quarks. Therefore in this theory baryons should be *degenerate* with appropriate mesons. It reminds us of what we are used to in supersymmetric (SUSY) QCD, however, these degenerate baryons and mesons form different representations of flavor and spin groups, and therefore their numbers do *not* match. So PGSY QCD is a kind of intermediate case between SUSY QCD and ordinary QCD, in which no relation between baryons and mesons exists. As the real world with $N_c = 3$ is in between the two extremes $N_c = 2$ and $N_c = \infty$, the former case deserves to be studied in details. (Furthermore, we will speculate below that the real world is probably even closer to the former rather than the latter extreme.)

In the $N_c = 2$ theory the lowest (scalar) baryon (or diquark) is bound as strongly as the lowest meson, the massless pion. (Furthermore, as we discuss below such strong binding also ensures a very small size of this baryon.) The general pattern of symmetry breaking is $SU(2N_f) \to Sp(2N_f)$ and the number of Goldstone modes is

$$N_{\text{Goldstone}} = 2N_f^2 - N_f - 1 \tag{67}$$

Let us mention three cases specifically. For $N_f = 1$ there is *no* Goldstone boson‡. For the most interesting case of $N_f = 2$ the coset (ratio) of the full group over the remaining one is

$$K = SU(4)/Sp(4) = SO(6)/SO(5) = S^5 \tag{68}$$

which means the five dimensional sphere with 5 massless modes: three of those are pions, plus the scalar diquark S and its anti-particle $\bar{S}$. The next case, $N_f = 3$, leads to 14 Goldstone bosons. It is easy to count them: mesons form the usual $SU(3)_F$ octet, plus 3 diquarks and and 3 anti-diquarks belonging to the $\underline{3}$ and 3 representations, because flavor indices are convoluted with ϵ_{ijk}, and so on.

Let us now consider properties of this theory at non-zero density or chemical potential μ. Unlike other QCD-like theories, the two color case allows for straightforward studies on the lattice because the fermionic determinant remains real even for non-zero μ. Nevertheless, very little work was done to take advantage of this fact.

As we have already mentioned in the introduction, the first numerical studies of the instanton liquid model for finite density have been recently performed by T. Schaefer[73]. Among his results, there are those for the $N_c = 2$ theory: it was also found that $< \bar{\psi}\psi >$ starts decreasing with μ only above some critical value

$$\mu_c \approx (mK)^{1/2} \tag{69}$$

Here m is the quark mass and§ $K \approx 1.2$ GeV. (Note that in QCD $K = m_\pi^2/(m_u+m_d) \approx 1.7$ GeV.) Dependence of the mesonic condensate on μ above μ_c was found to be similar to what was seen on the lattice. The diquark condensate and density was not studied in this work.

Let us now review general features expected on theoretical grounds, starting for simplicity with the *massless* $N_c = N_f = 2$ theory. The usual vacuum state has a standard chiral symmetry breaking pattern, with a non-zero value of the "mesonic" condensate $< \bar{q}q >= n_0 \sim \Lambda^3$, like in QCD. There are five massless Goldstone bosons mentioned above. Rotations on the five dimensional sphere along Goldstone directions cost no energy, and by doing so in the direction of the scalar diquark one naturally obtains states with the diquark density from zero to n_0. As it energetically costs nothing, the chemical potential $\mu = \partial E/\partial n_q = 0$, till the maximal density $n_q = 2n_0$ is reached. At this point chiral symmetry gets restored, $< \bar{q}q >= 0$, the five Goldstone bosons are now the pions, sigma and $\bar{S}$. What is very important, the scalar diquark

‡Recall that due to the U(1) anomaly, even the corresponding meson, η', is massive. The diquark, similar to what we need, cannot even exist due to the Pauli principle.

§The units are defined by setting the instanton density to be exactly 1 fm^{-4}.

acquires the role of the former sigma meson, and therefore becomes massive. The reason for this is, as usual, repulsive interaction with particles in the condensate.

If one increases the density further, the system is still a Bose condensate of diquarks. However, the energy starts to grow and the non-zero chemical potential appears. The next qualitative phenomenon¶ occurs when half of the diquark chemical potential reaches the quark mass, $\mu_S/2 = m_q$: from now on the system is a Bose-Fermi mixture of diquarks and quarks. Equilibrium demands that both components have the same chemical potential.

It is convenient to demonstrate first how it works for non-zero quark mass using the simplest effective Lagrangian, an analog of the linear sigma model. Together with the usual kinetic energy terms, it has a potential

$$V = \lambda(\vec{\pi}^2 + \sigma^2 + S^2 + \bar{S}^2 - v^2)^2 - A\sigma - \mu^2 S^2 \tag{70}$$

where we have also included the chemical potential for the diquark and and the chiral symmetry breaking mass term. At $\mu = 0$ one obviously gets all the usual results, in particular the Goldstone mass $m_g^2 = A/v$, the sigma mass $m_\sigma^2 = 8\lambda v^2$, etc. For non-zero μ a (mean field) minimization over S produces the equation for its mean value $< S >$

$$4\lambda < S > (\sigma^2 + < S >^2 - v^2) = 2\mu^2 < S > \tag{71}$$

It is therefore either zero (and we are back to the vacuum solution) or

$$< S >^2 = v^2 + \frac{\mu^2}{\lambda} - \frac{A^2}{16\mu^2} \tag{72}$$

Putting it back into the effective energy density one finds for the unusual vacuum

$$\epsilon_{<S>} = -\mu^2 v^2 - \frac{3A^2}{16\mu^2} \tag{73}$$

to be compared to that for the usual vacuum

$$\epsilon_{<\sigma>} = -m_g^2 v^2 + \frac{m_g^4}{16\lambda} \tag{74}$$

It clearly wins if μ is about (but not exactly!) the pion mass. Furthermore, differentiating our effective energy‖ over μ leads to

$$n = 2\mu v^2 - \frac{3m_g^2 v^2}{8\mu^3} \tag{75}$$

(Recall that it can only be used above the transition, at not too small a μ.) The behavior of the mesonic condensate in this phase is

$$< \sigma > = \frac{m_g^2 v}{4\mu^2} \tag{76}$$

which is roughly consistent with lattice data behavior above the critical μ.

Finally, let us look at the *mass* of the diquark. Taking for simplicity the massless ($A = 0 = m_g$) case, one can easily compute from the effective action that it is given by

¶Assuming that deconfinement has also happened at about the same conditions as chiral restoration.

‖It is worth recalling that it is actually $\epsilon_{\text{eff}} = \epsilon - \mu n$ where ϵ is the true energy and n is the density. Therefore true energy is positive and grows with μ.

$m_S = (8\lambda v^2 + 10\mu^2)^{1/2}$, growing from the value which the sigma meson has at $\mu = 0$. As we commented above, after it reaches twice the quark mass the diquarks become unstable against decay and one should populate both diquark Bose gas and quark Fermi gas in order to prevent this.

It brings us to the next important issue, properties of *single* quarks propagating in this matter. Generally, it can only be discussed at high enough density, in the deconfined phase. However, most chiral models (including versions of sigma, NJL or instanton-based models, which we will eventually discuss) disregard confinement, producing instead a finite "constituent" quark mass in the vacuum. For the massless theory, symmetry arguments suggest that rotation in our multi-dimensional chiral circle from the usual vacuum with non-zero $< \sigma >$ to the unusual one with non-zero $< S >$ should not change the quark mass value. At the same time, chiral symmetry should be restored in this new vacuum, so the mass should be a "chiral" one. It means that the quark propagator in momentum space should look like

$$S(p) = \frac{p_\mu \gamma_\mu}{p^2 - m_{\text{eff}}^2}. \tag{77}$$

This is indeed the case, as one can see from explicit diagrams: only even number of condensed diquark insertions are allowed in "normal" Green functions.

Let us now return to the real world with $N_c = 3$. The scalar diquark, according to instanton liquid calculations[8] is much lighter than all others, with a mass of about 500 MeV (to be compared with twice the constituent quark mass 700-800 MeV). It is plausible that there exists a "diquark condensate" phase as an intermediate between nuclear matter and the single-quark Fermi gas. What is definitely clear, at *any* density some analog of diquarks exists, now in form of "Cooper pairs" living on the surface of the Fermi sphere: as known from the Bardeen-Cooper-Schrieffer theory of superconductivity, arbitrary small attraction leads to binding. In the instanton ensemble it should look like "polymers" made of alternating instantons and anti-instantons**, local in space and extended indefinitely in the time direction. First indications for existence of these structures have indeed been seen in[73].

Diquarks provide a double advantage over a quark Fermi gas, due to binding $m_{dq} < 2m_q$ and their Bose condensation. However, it would be wrong to assume that any number of diquarks can be put into the $p = 0$ state: diquarks are composite objects and, like nucleons, they should have a repulsive "core". We have accounted for this effect by introducing a scattering length $a \approx .3$ fm into the expression for the energy of the diquark Bose gas (counted per *quark*)

$$\frac{\epsilon^B}{n_q} = \frac{4\pi a n_{dq}}{m}[1 + \frac{128}{15\sqrt{\pi}}(a^3 n_{dq})^{1/2}] \tag{78}$$

where n_{dq} is the diquark density. The first term is the mean field result from condensed diquarks, like included in our sigma-model discussion above, and the second term (calculated by Lee and Yang in the 50's) comes from non-condensate diquarks. Repulsion makes the diquark Bose gas less favorable than some optimal Bose-Fermi mixture. Results of our calculations are shown in Fig. 9, in which matter consists of (i) diquark Bose gas, being in chemical equilibrium with (ii) blue-green quarks, and neutralized in color and electric charge by the appropriate amount of (iii) red quarks. For definiteness, we use a quark mass of 400 MeV and a diquark mass of 500 MeV.

In addition we have introduced the energy of color strings. In order to explain how we have done it, we recall an old puzzle: for $\bar{c}c, \bar{b}b$ quarkonia we have an excellent description with a standard Coulomb+linear potential, while for hadrons made

**Note the clear correlation with "molecules" we discussed above for high T phase.

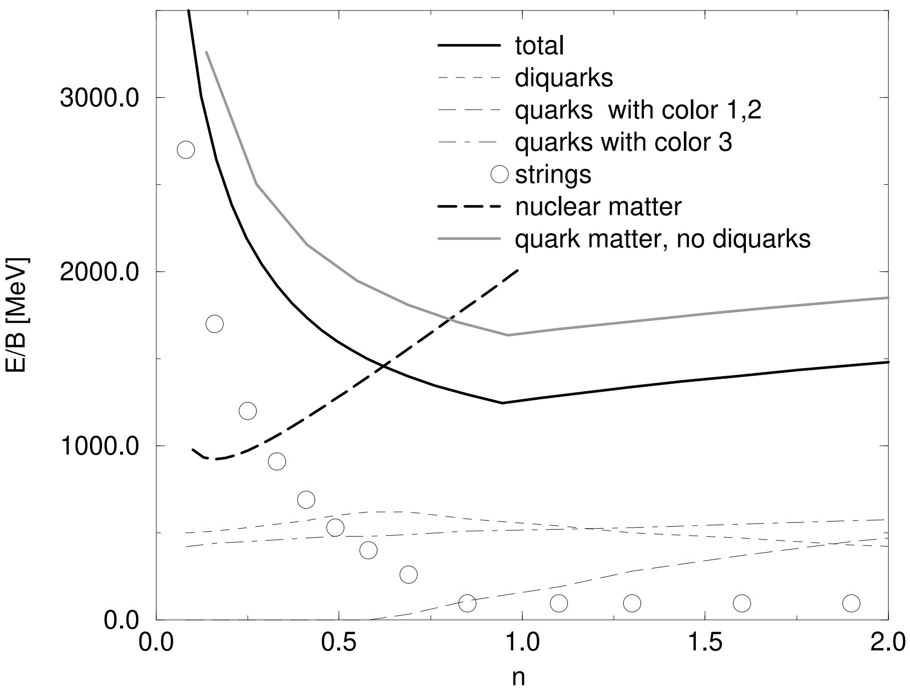

Figure 9. Energy per baryon (in MeV) versus baryon charge density n_b (fm^{-3}). Curves explained in the text.

of light quarks one uses a much weaker confining potential. (Many models like NJL and IILM even obtain correct hadronic masses without it: most of it just comes from the constituent quark mass.) The puzzle seems to be solved as follows: due to the extended nature of constituent quarks (as opposed to the point-like c or b ones), they have form-factors and interact only with sufficiently soft gluonic modes. On the lattice this effect was studied by measuring the string tension after smoothing the gauge fields: the resulting potential looks as

$$V = K|R - R_0|\theta(R - R_0) \tag{79}$$

with the standard string tension $K \approx 1$ GeV/fm and $R_0 \approx .7$ fm (see the example in[14]). In other words, a string seems to be formed only if constituent quarks do not overlap. We evaluate the average energy of a string schematically, substituting $R = n_{\mathrm{tot}}^{-1/3}$ where n_{tot} is the total density of all quarks and diquarks. As seen from the figure, it prevents nuclear matter from dissolution into a gas of diquarks and quarks. The latter obtains a shallow (meta-stable) minimum at a density around six times nuclear density. (Most probably, at such densities confinement forces disappear due to deconfinement phenomenon anyway.) Existence of the minimum may be an artifact of the crude model: the bottom-line is that diquarks allow for significant overall energy gain relative to the quark matter (upper grey curve), and they also make quark matter very "soft".

What is not taken into account in this model is the effect of diquark condensation on the vacuum ($< \bar{q}q >$) and on the dispersion relation of the "blue-green" quarks. (The latter may be justified by the fact that at $n_b \sim 1$ fm^{-3} their role is not yet large.)

Phases of QCD with more quark flavors

In this section we discuss further the role of quarks in QCD, adding more flavors to it. If we add too much of them, namely $N_f > 33/2$ (here and below we imply 3

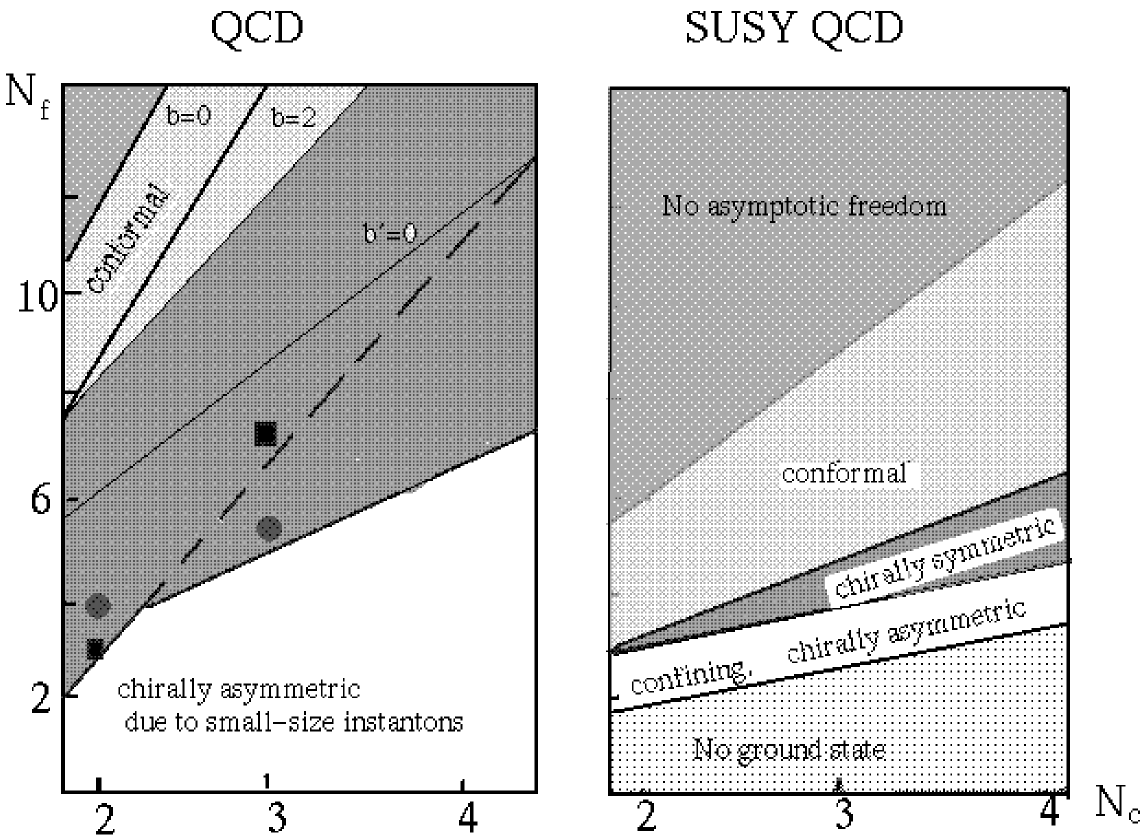

Figure 10. Schematic phase diagram of zero T QCD (a) and supersymmetric QCD (b) as a function of the number of colors N_c and the number of flavors N_f. Squares show where lattice calculations have found the infrared fixed point, dots are where the instanton ensemble is purely "molecular", with the unbroken chiral symmetry.

colors), the asymptotic freedom is lost and we get an *uninteresting* field theory with a charge growing at small distances, basically a theory as bad as QED! So our "most flavored" QCD is with 16 flavors, and we work our way down from there (see Fig. 10). The phase we are in at that point is actually a rather simple one, known as the Banks-Zaks conformal domain[56]. It has an infrared fixed point at small coupling $g_*^2/16\pi^2 = -b/b' << 1$ (b, b' are the one and two-loops coefficients of the beta function). It happens in the perturbative domain, so the charge is small both at small and large distances. There are no particles in this phase, and all correlators decay as powers of the distance. In this phase the non-perturbative phenomena like instantons are exponentially suppressed, $\exp(-\mathrm{const}/g_*^2)$. However, as one lowers the fermion number, the fixed point g_*^2 moves to larger values and eventually disappears. Lattice simulations of multi-flavor QCD were recently reported in[57]. These authors studied QCD with up to 240 flavors. Studying the sign of the beta function in the weak and strong coupling domains, they confirmed the existence of an infrared fixed point as low as at $N_f = 7$.

It is not known which phase we find next at $N_f = 5 - 6$, most probably it is the so called Coulomb phase (basically QGP).

The results of the interacting instanton model are summarized by Fig. 11, which shows how one singular point at $N_f = 2$ develops into the discontinuity line for $N_f = 3$. The value of T_c goes down with increasing N_f and at $N_f = 5$[††] one finds that the

[††]Note that the $N_f = 4$ case is missing. It is because I have found the condensate to be small and comparable to finite-size effects. In order to separate those one should do calculations in different boxes, which is time consuming.

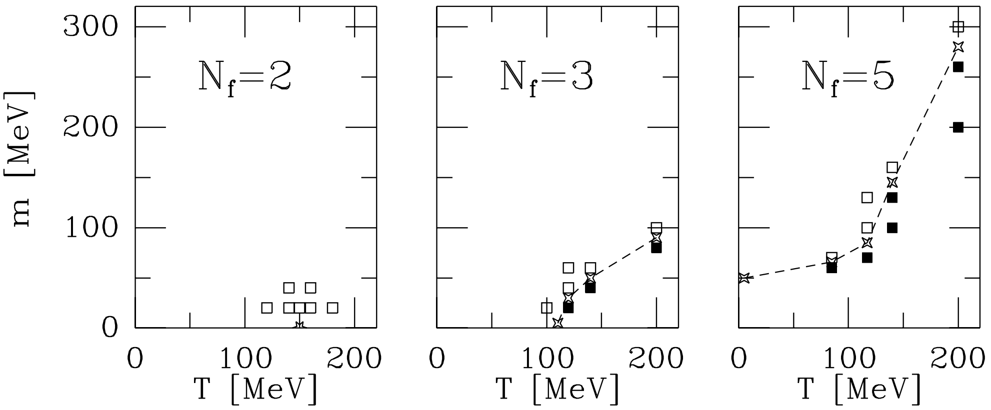

Figure 11. Phase diagram (temperature-quark mass plane) of the instanton liquid for different numbers of quark flavors, N_f=2, 3 and 5. The open squares indicate a non-zero chiral condensate, while solid ones indicate that it is zero. The dashed lines show the approximate location of the discontinuity line.

chiral symmetry is restored even at $T = 0$, provided quarks are light enough. New lattice results from the Columbia group (R. Mawhinney, private communication) deal with QCD with $N_f = 4$. When the measured masses are extrapolated to small quark masses, $m \to 0$, it was found that a dramatic and significant drop in chiral symmetry breaking effects occurs: the $\pi - \sigma, \rho - a_1, N - N^*(1/2^-)$ splittings are much smaller than for $N_f = 0-3$, studied before. It suggests that chiral restoration is indeed nearby, similarly to what was found in the instanton calculations.

Now we return to Figure 10, and explain its rhs, showing a similar phase diagram for the $N = 1$ SUSY QCD based on[58]. Not going into details, let me only mention that the vacuum is now definitely dominated by instanton-antiinstanton molecules, and their contribution can be calculated without problems (in QCD there are large perturbative contributions). There are two phases which are impossible in QCD: a case without a ground state (molecules force the system toward infinite Higgs VEV) and also a funny situation with unbroken chiral symmetry and confinement (hadrons exist but are degenerate in parity). It is amusing that chiral symmetry is restored at $N_f = N_c + 1$, similar to what was found in QCD in the instanton model. Also note, that in this case the existence of the Coulomb phase is a proven fact.

Finally, let me comment that nowhere the role of instantons is more clearly seen than in the supersymmetric theories. With the perturbative contributions basically cancelled out, there is no longer a problem to separate instantons from the perturbation series. For example, for $N = 2$ extended supersymmetric QCD general constraints are so powerful that Witten and Seiberg have been able to determine not just the effective potential, but the complete low energy effective action[59]. Its expansion shows powers of the instanton densities only, suggesting those to be the sole dynamical features. Furthermore, if the Higgs VEV a is large ($a \gg \Lambda$), the semi-classical description is valid, instantons are small $\rho \sim a^{-1}$ and the instanton ensemble is dilute $n\rho^4 \sim \Lambda^4/a^4 << 1$. One can then calculate the first and the second order effects in density[60, 61, 62], and the results have explicitly reproduced the Witten-Seiberg expansion. Not only individual diagrams are all well convergent, but the instanton-based series seem to be convergent as well, explaining where and why the monopole mass vanishes. Furthermore, one can work out[63] a correct large N_c limit of the $N = 2$ theory, finding that (contrary to naive expectations) the instantons are not suppressed. It would be interesting to see what the instanton contribution is to the $N = 2$ theory for other terms in the effective

Lagrangian (with more derivatives than in the Seiberg-Witten result), or for $N = 1$ theories, bridging the gap between $N = 0$ QCD and the $N = 2$ theory.

Acknowledgments

These lectures are based on works done with my collaborators, especially with T. Schaefer and J. Verbaarschot, who contributed immensely to progress reported in them. I am very grateful to Pierre van Baal, the major organizer of this school, for the wonderful opportunity to learn more about new developments in field theory.

REFERENCES

1. Y. Nambu and G. Jona-Lasinio, *Phys. Rev.*, 122:345, 1961.
2. T. Schäfer and E. V. Shuryak, 1996, Instantons in QCD, hep-ph/9610451, Rev.Mod.Phys, in press.
3. T. Schäfer and E. V. Shuryak, *Phys. Rev. Lett.*, 75:1707, 1995.
4. E. V. Shuryak, *Nucl. Phys.,*, B198:83, 1982.
5. D. I. Diakonov and V. Yu. Petrov, *Nucl. Phys.*, B272:457, 1986.
6. G. 't Hooft, *Phys. Rep.*, 142:357, 1986.
7. E. V. Shuryak, *Nucl. Phys.*, B203:93, 1982.
8. T. Schäfer, E. V. Shuryak, and J. J. M. Verbaarschot, *Nucl. Phys.*, B412:143, 1994.
9. S. Chernyshev, M. A. Nowak, and I. Zahed, hep-ph/9510326.
10. E. V. Shuryak, *Rev. Mod. Phys.*, 65:1, 1993.
11. M. C. Chu, J. M. Grandy, S. Huang, and J. W. Negele, *Phys. Rev.*, D 48:3340, 1993.
12. E. Shuryak, *Phys. Lett.*, 107B:103, 1981.
13. H. Georgi and A. Manohar, *Nucl. Phys.*, B234:189, 1984.
14. M. Feurstein, E. M. Ilgenfritz, M. Muller-Preussker and S. Thurner, hep-lat/9611024.
15. M. C. Chu, J. M. Grandy, S. Huang, and J. W. Negele, *Phys. Rev.*, D49:6039, 1994.
16. T. DeGrand, R.L. Jaffe, K. Johnson, and J. Kiskis, *Phys. Rev.*, D12:2060, 1975.
17. E. V. Shuryak, *Phys. Lett.*, B79:135, 1978.
18. M. C. Chu, J. M. Grandy, S. Huang, and J. W. Negele, *Phys. Rev. Lett.*, 70:225, 1993.
19. R. Rajaraman, *Solitons and Instantons*, North Holland, Amsterdam, 1982.
20. M. Shifman, *Instantons in Gauge Theories*, World Scientific, Singapore, 1994.
21. A. A. Belavin, A. M. Polyakov, A. A. Schwartz, and Yu. S. Tyupkin, *Phys. Lett.*, 59B:85, 1975.
22. G. 't Hooft, *Phys. Rev.*, D14:3432, 1976.
23. D. I. Diakonov and V. Yu. Petrov, *Phys. Rev.*, D50:266, 1994.
24. M. A. Shifman, A. I. Vaishtein, and V. I. Zakharov, *Phys.Lett.*, B76:971, 1978.
25. M. A. Shifman, A. I. Vainshtein, and V. I. Zakharov, *Nucl. Phys.*, B147:385, 448, 1979.
26. E. Witten, *Nucl.Phys.*, B156:269, 1979.
27. G. Veneziano, *Nucl.Phys.*, B159:213, 1979.
28. C. Michael and P. S. Spencer, *Phys. Rev.*, D52:4691, 1995.
29. E. V. Shuryak, *Phys. Rev.*, D52:5370, 1995.
30. M. I. Polikarpov and A. I. Veselov, *Nucl. Phys.*, B297:34, 1988.
31. C. Michael and P. S. Spencer, *Nucl. Phys. (Proc. Suppl.)*, B42:261, 1995.
32. S. L. Adler, *Phys. Rev.*, 177:2426, 1969.
33. J. S. Bell and R. Jackiw, *Nuovo. Cim.*, A60:47, 1969.
34. V. N. Gribov, 1981, KFKI-1981-66 preprint, Budapest.
35. M. A. Shifman, *Sov. Phys. Usp.*, 32:289, 1989.
36. G. 't Hooft, *Phys. Rev. Lett.*, 37:8, 1976.
37. M.A. Shifman, A.I. Vainshtein, and V.I. Zakharov, *Nucl.Phys.*, B163:46, 1980.
38. T. Schäfer and E. V. Shuryak, *Phys. Rev*, D53:6522, 1996.
39. E. V. Shuryak and J. J. M. Verbaarschot, *Phys. Rev.*, D52:295, 1995.
40. E. V. Shuryak and J. J. M. Verbaarschot, *Nucl. Phys.*, B410:55, 1993.
41. T. Schäfer, E. V. Shuryak, and J. J. M. Verbaarschot, *Phys. Rev.*, D51:1267, 1995.
42. E. V. Shuryak, *Nucl. Phys.*, B203:116, 1982.
43. E. V. Shuryak and J. L. Rosner, *Phys. Lett.*, B218:72, 1989.
44. B. L. Ioffe, *Nucl. Phys.,*, B188:317, 1981.
45. V. M. Belyaev and B. L. Ioffe, *Sov. Phys. JETP,*, 83:976, 1982.

46. A. E. Dorokhov and N. I. Kochelev, *Z. Phys.*, C 46:281, 1990.
47. H. Forkel and M. K. Banerjee, *Phys.Rev.Lett.*, 71:484, 1993.
48. P. van Baal and A. S. Kronfeld, *Nucl. Phys. B (Proc. Suppl.)*, 9:227, 1989.
49. K. Ishikawa, G. Schierholz, H. Schneider, and M. Teper, *Phys.Lett.*, 128B:309, 1983.
50. F. de Forcrand and K.-F. Liu, *Phys. Rev. Lett.*, 69:245, 1992.
51. S. Narison, *Z. Phys.*, C26:209, 1984.
52. E. Bagan and S. Steele, *Phys. Lett.*, B243:413, 1990.
53. E.-M. Ilgenfritz and E. V. Shuryak, *Phys. Lett.*, B325:263, 1994.
54. E. Shuryak and M. Velkovsky, Mean field approach to instanton effects close to the phase transition, hep-ph/9603234.
55. I.I. Balitsky and A. V. Yung, *Nucl. Phys.*, B274:475, 1986.
56. T. Banks and A. Zaks, *Nucl. Phys.*, B82:196, 1982.
57. Y. Iwasaki, K. Kanaya, S. Kaya, S. Sakai, and T. Yoshie, *Z. Phys.*, C71:343, 1996.
58. N. Seiberg, *Phys. Rev.*, D49:6857, 1994.
59. N. Seiberg and E. Witten, *Nucl. Phys.*, B426:19, 1994.
60. D. Finnel and P. Pouliot, *Nucl. Phys.*, B453:225, 1995.
61. K. Ito and N. Sasakura, *Phys. Lett.*, B382:95, 1996.
62. N. Dorey, V.V. Khoze, and M.P. Mattis, *Phys. Rev.*, D54:2921, 1996.
63. M.R. Douglas, S.H. Shenker, Nucl.Phys.B447:271-296,1995; hep-th/9503163.
64. P. Kim (CLEO), Talk at FCNC 1997, Santa Monica, CA (Feb 1997).
65. E. Shuryak and A. Zhitnitsky, The gluon/charm content of the η' meson and instantons, hep-ph/9706316.
66. I. Halperin and A. Zhitnitsky, $B \to \eta' + K$ decay as a unique probe of η meson, hep-ph/9704412.
67. M.Shifman, Z.Phys.C4 (1980) 345.
68. J.D. Bjorken, CP and B Physics: Progress and Prospects, hep-ph/9706524.
69. S.J. Brodsky, P. Hoyer, A.H. Mueller and W.-K. Tang, Nucl.Phys. B369 (1992) 519; S. J. Brodsky, Beyond standard QCD, hep-ph/9503391.
70. R. Rapp, E. Shuryak and M. Velkovsky, High density matter and instantons, NTG-SUNY preprint, 1997.
71. M. Anselmino et al, Rev.Mod.Phys. 65 (1993) 1199.
72. W. Pauli, Nuovo Cim. 6 (1957) 205; F. Gursey, ibid 7 (1958) 411.
73. T. Schaefer, Instantons and the chiral phase transition at non-zero baryon density, hep-ph/9708256.